

1990

A geophysical study of the hydrogeology of the Carrizo Plain area, San Luis Obispo County, California

Jon W. Cooper
San Jose State University

Follow this and additional works at: https://scholarworks.sjsu.edu/etd_theses

Recommended Citation

Cooper, Jon W., "A geophysical study of the hydrogeology of the Carrizo Plain area, San Luis Obispo County, California" (1990).
Master's Theses. 3252.

DOI: <https://doi.org/10.31979/etd.2yuu-aymx>
https://scholarworks.sjsu.edu/etd_theses/3252

This Thesis is brought to you for free and open access by the Master's Theses and Graduate Research at SJSU ScholarWorks. It has been accepted for inclusion in Master's Theses by an authorized administrator of SJSU ScholarWorks. For more information, please contact scholarworks@sjsu.edu.

INFORMATION TO USERS

The most advanced technology has been used to photograph and reproduce this manuscript from the microfilm master. UMI films the text directly from the original or copy submitted. Thus, some thesis and dissertation copies are in typewriter face, while others may be from any type of computer printer.

The quality of this reproduction is dependent upon the quality of the copy submitted. Broken or indistinct print, colored or poor quality illustrations and photographs, print bleedthrough, substandard margins, and improper alignment can adversely affect reproduction.

In the unlikely event that the author did not send UMI a complete manuscript and there are missing pages, these will be noted. Also, if unauthorized copyright material had to be removed, a note will indicate the deletion.

Oversize materials (e.g., maps, drawings, charts) are reproduced by sectioning the original, beginning at the upper left-hand corner and continuing from left to right in equal sections with small overlaps. Each original is also photographed in one exposure and is included in reduced form at the back of the book.

Photographs included in the original manuscript have been reproduced xerographically in this copy. Higher quality 6" x 9" black and white photographic prints are available for any photographs or illustrations appearing in this copy for an additional charge. Contact UMI directly to order.

U·M·I

University Microfilms International
A Bell & Howell Information Company
300 North Zeeb Road, Ann Arbor, MI 48106-1346 USA
313 761-4700 800 521-0600



Order Number 1340505

**A geophysical study of the hydrogeology of the Carrizo Plain
area San Luis Obispo County, California**

Cooper, Jon W., M.S.

San Jose State University, 1990

U·M·I
300 N. Zeeb Rd.
Ann Arbor, MI 48106



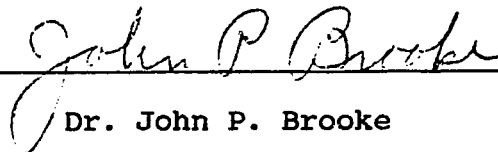
A GEOPHYSICAL STUDY
OF THE
HYDROGEOLOGY OF THE CARRIZO PLAIN AREA
SAN LUIS OBISPO COUNTY, CALIFORNIA

A Thesis
Presented to
The Faculty of the Department of Geology
San Jose State University

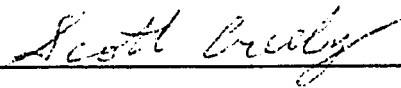
In Partial Fulfillment
of the Requirements for the Degree
Master of Science

By
Jon W. Cooper
May, 1990

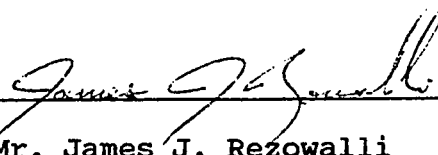
APPROVED FOR THE DEPARTMENT OF GEOLOGY



Dr. John P. Brooke

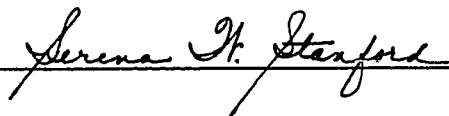


Dr. Scott Creely



Mr. James J. Rezowalli

APPROVED FOR THE UNIVERSITY



ABSTRACT

A GEOPHYSICAL STUDY OF THE HYDROGEOLOGY OF THE CARRIZO PLAIN AREA, SAN LUIS OBISPO COUNTY, CALIFORNIA

by Jon W. Cooper

This investigation was conducted to locate structural geologic features and variations in aquifer characteristics in an area within the Carrizo Plain, San Luis Obispo County, California. The investigation included a review of the established geologic knowledge for the region, followed by field studies. The field studies included surface magnetometer surveys, thermal borehole logging, and a piezometric level survey. Existing borehole electric logs were obtained. The conclusions of the investigation were then derived from a collective interpretation.

The investigation concluded that a fault extends beneath the valley fill in the northwestern part of the area, and that a subsurface basaltic dike is located in the southeastern part of the area. The valley was determined to have a deep aquifer overlain by a confining clay-rich layer in the central part of the area. Areal and depth-related variations in water quality are influenced by the presence of evaporites near Soda Lake and in the region near the San Andreas fault.

ACKNOWLEDGEMENTS

The assistance of several people was important to this investigation. Mr. Jerry Diefenderfer helped design a project which would benefit San Luis Obispo County. Mr. Tim Cleath and Miss Leah Cooper were most helpful in reviewing and editing transcripts. Mr. Chuck Pritchard's contribution of special materials improved the quality of the study. Mr. Clint Milne's patience in expediting county government procedures was greatly appreciated. Thanks also are due the authorized personnel at the Los Angeles office of the California Department of Water Resources and at the Menlo Park office of the United States Geological Survey for cheerfully assisting in the research. Dr. John Brooke, Dr. Scott Creely, Dr. June Oberdorfer, Dr. Joe Birman, and Mr. Jim Rezowalli were all helpful and encouraging at various stages of the investigation. Much gratitude and appreciation go to all these people, to the taxpayers of San Luis Obispo County for their financial support, and to Jan, for her encouragement during the many hours spent on the project.

TABLE OF CONTENTS

	Page
ABSTRACT.....	iii
INTRODUCTION.....	1
Purpose.....	1
Location.....	1
Climate and Hydrology.....	3
REVIEW OF LITERATURE.....	5
REGIONAL GEOLOGY.....	6
Geomorphology.....	6
Geologic Setting.....	7
Tectonic Setting.....	11
STRATIGRAPHY.....	14
Basement Complex.....	14
Simmler Formation.....	14
Vaqueros Formation.....	15
Soda Lake Shale Member.....	15
Painted Rock Sandstone Member.....	15
Monterey Shale.....	16
Saltos Shale Member.....	16
Whiterock Bluff Shale Member.....	17
Branch Canyon Sandstone.....	17
Basalt.....	17
Santa Margarita Formation.....	18

Paso Robles Formation.....	13
Surficial Deposits.....	19
STRUCTURE.....	20
METHODS, RESULTS AND INTERPRETATIONS.....	21
Magnetic Method.....	21
Magnetic Investigation.....	21
Interpretation of Magnetics.....	26
Thermal Logging Method.....	40
Thermal Logging Results.....	42
Interpretation of Thermal Logs.....	52
Method of Wireline Logging of Boreholes.....	54
Wireline Logging Results and Interpretation.....	55
Piezometric Levels.....	65
DISCUSSION.....	70
CONCLUSIONS.....	73
BIBLIOGRAPHY.....	74

LIST OF ILLUSTRATIONS

Figure	Page
1. Location Map.....	2
2.1 Geologic Map.....	8
2.2 Explanation of Symbols.....	9
3. Map of Magnetometer Lines and Wells.....	23
4. Magnetic Contour Map.....	25
5.1 Magnetic Profile of Line 9.....	27
5.2 Computer Model of Anomaly.....	32
5.3 Magnetic Profile of Line 8.....	33
5.4 Magnetic Profile of Line 4.....	35
5.5 Magnetic Profile of Line 5.....	36
5.6 Magnetic Profile of Line 6.....	37
5.7 Magnetic Profile of Line 7.....	38
5.8 Magnetic Profile of Lines 1,2, and 3.....	39
6.1 Thermal Log of Well Number 3.....	44
6.2 Thermal Log of Well Number 5.....	46
6.3 Thermal Log of Well Number 4.....	47
6.4 Thermal Log of Well Number 7.....	49
6.5 Thermal Log of Well Number 8.....	50
6.6 Thermal Log of Well Number 2.....	51
7.1 Electric Log of Well Number 1.....	56
7.2 Electric Log of Well Number 3.....	57
7.3 Electric Log of Well Number 5.....	60

7.4 Electric Log of Well Number 6.....	62
7.5 Electric Log of Well Number 7.....	64
8. Map of Piezometric Surface Contour.....	66
9. Well Identification System.....	69

LIST OF TABLES

Table	Page
1. Magnetometer Lines.....	24
2. Magnetic Susceptibilities of Samples.....	29
3. Thermal Conductivities of Rocks.....	41
4. Water Well Identification.....	43
5. Piezometric Levels.....	67

INTRODUCTION

Purpose

The purpose of the investigation was to locate structural features and variations in aquifer characteristics which are not readily detectable on the surface of the recent valley sediments, and to relate their significance to the area's hydrogeology. Magnetic survey data, water well measurements, and well logs of selected locations of the Carrizo Plain, California, were evaluated. The location for the investigation was chosen to include residential lots in California Valley, and an area of the Carrizo Plain with a history of irrigation. Field data were collected, evaluated, analyzed, and correlated to previous work on regional geology, faulting, stratigraphy, and related studies.

Location

The area of investigation is located in eastern San Luis Obispo County, California, approximately midway between Los Angeles and San Francisco (Figure 1). It comprises approximately 51 square miles in townships 29 south and 30 south and ranges 18 east and 19 east, Mount Diablo base and meridian. The area of investigation is included in the United States Geological Survey Simmler, Calif. and California Valley, Calif. 1:24000-scale topographic maps.

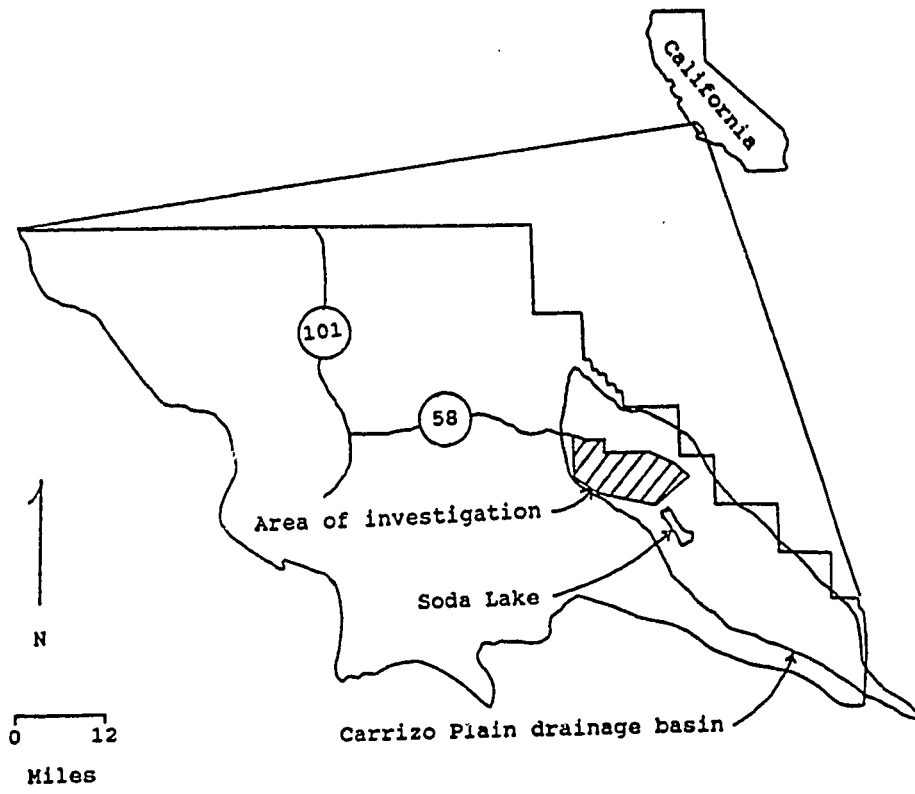


Figure 1. Map showing the location of San Luis Obispo County and the area of investigation.

California highway 58 delineates the northern border, which begins seven miles to the west of Simmler and ends seven miles to the east of Simmler, at the San Andreas fault. The southernmost part of the site is 7.5 miles south from highway 58 on Soda Lake Road, at its intersection with Seven-Mile Road. Seven-Mile Road forms the southeastern border. Located 1.5 miles southward from highway 58 on Soda Lake Road is the village of California Valley. A motel, restaurant, and fire station are located within this 7000-lot subdivision which occupies approximately the eastern half of the area of investigation.

Climate and hydrology

The Carrizo Plain is in an area of Steppe climate, and is described as having hot days and cool nights in the summer. The winters are classified as "keen days with pleasant wind effects, the nights cold with cold wind chill" (Eichel, 1971). Annual rainfall is locally variable from approximately eight inches to 10.5 inches (Lima, 1975).

The Carrizo Plain basin is one of six hydrogeologic units of San Luis Obispo County, as designated by the California Department of Water Resources (Bulletin 18, 1958). All surface runoff within the basin flows into Soda Lake. The drainage basin was estimated to comprise an area of approximately 416 square miles. Within the basin are

approximately 350 square miles of post-Pliocene water-bearing alluvium (Kemnitzer, 1967).

REVIEW OF LITERATURE

The most comprehensive hydrogeologic study of the Carrizo Plain area was written by Kemnitzer (1967). This study addresses the difficulties of ground water development and its maximum future potential within the area. The study is a source of information concerning ground water recharge and discharge, groundwater quality, movement, and accumulation. It has not been published, but at the time of this writing it has been placed in the special collections section of the library at California State Polytechnic University in San Luis Obispo, California. The study is also on file at the San Luis Obispo County engineering department.

There are several detailed studies of the stratigraphy and structural geology of the area. Dibblee (1973) wrote the most local generalized description. Galehouse (1967) produced a thorough assessment of paleocurrents within the Paso Robles Formation, and Lagoe (1985) discussed depositional environments of the Monterey Shale in the Cuyama basin, an area near the Carrizo Plain. Surface seismic reflection work has been completed by various oil companies in the area.

REGIONAL GEOLOGY OF THE CARRIZO PLAIN AREA

Geomorphology

The study area is located within the Carrizo Plain, which is a structural basin. The southeastern end of the basin is located at the juncture of the Temblor Range to the northeast and the Caliente Range to the southwest. The elevation of the Temblor Range is 3,000 feet, and the elevation of the Caliente Range decreases from 4,000 feet at the southeastern end to 2,500 feet at the northwestern end. The basin extends approximately forty miles northwestward between these ranges and is approximately ten miles in width. The basin floor slopes southeastward from 2,100 feet in elevation at the north end to 1,940 feet in elevation at Soda Lake, a slope of approximately ten feet per mile. Soda Lake is a prominent desert playa within the basin which receives flood waters during wet seasons. It occupies approximately 3,000 acres in the central, low part of the basin.

The study area is bounded to the east by the San Andreas fault, which is a well-defined linear escarpment along the base of the Temblor Range. The eastern half of the study area contains a grid of graveled and unpaved roads which serve approximately 100 families living in the California Valley subdivision. The southwest border is

located along the base of the foothills and terminates at Syncline Hill. Syncline Hill consists of a syncline extending approximately 400 feet above the basin floor. The northwestern part of the study area is mostly non-irrigated grain cropland. At the time of this study approximately 160 acres were irrigated.

The topography and soils include rolling hills in the eastern part of the study area which expose Pleistocene anticlines of Paso Robles Formation which rise above the recent sediments (Figure 2.1). Soils in the western half of the area support non-irrigated small grain crops. Agriculture in the eastern half is mostly sheep and cattle grazing. This is due partly to the declining rainfall amounts to the east and partly to the accumulation of alkali in the soils, which makes grain production difficult.

Geologic setting

The San Andreas fault is the dominant geological feature of the Carrizo Plain. Northeast of the fault, Cretaceous to Recent sediments rest on Franciscan basement rocks of Jurassic and Cretaceous age. Southwest of the fault, within the area of investigation, the Cretaceous to Recent sediments overlie Santa Lucia Granodiorite of Late Cretaceous age. The granodiorite is intruded into metamorphic rocks of the Sur Series (Galehouse, 1967).

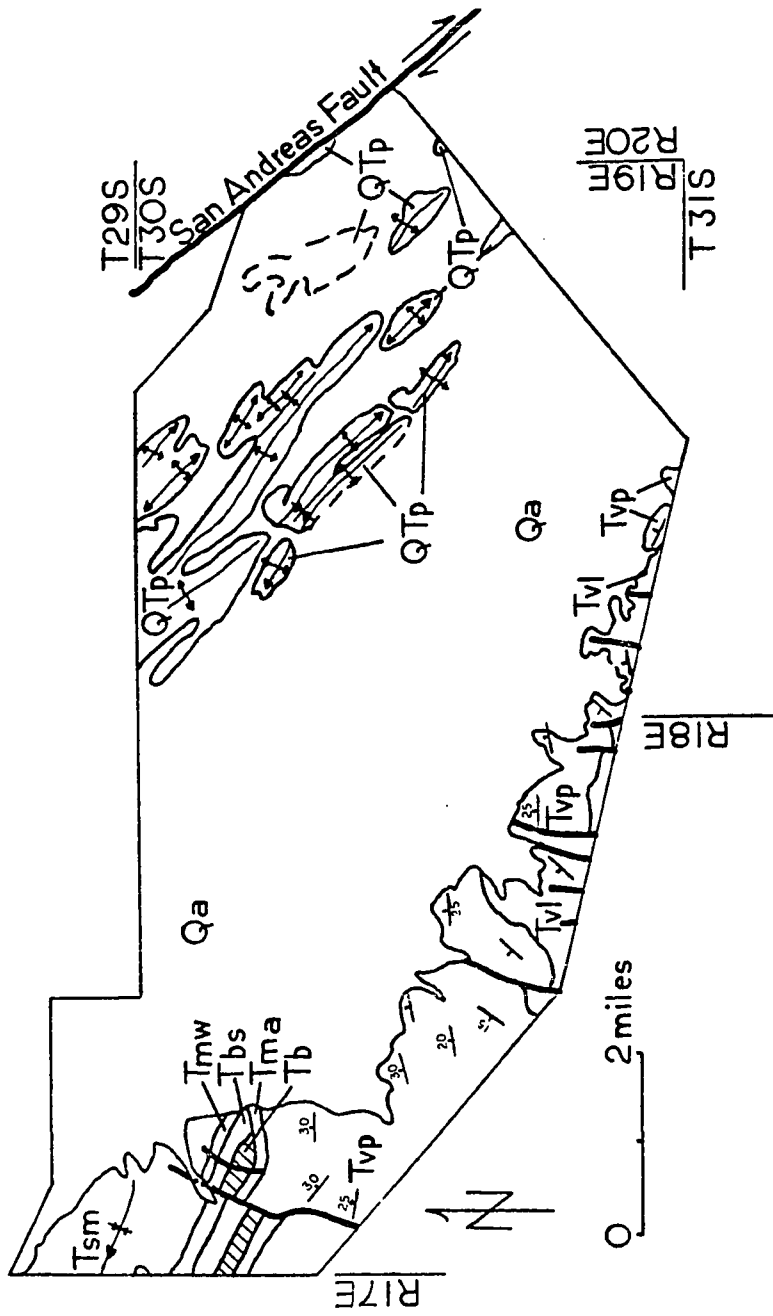


Figure 2.1. Geologic map of the area of investigation (modified from Dibblee, 1973). Legend: Figure 2.2.

LEGEND

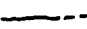
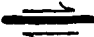
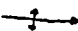
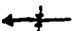
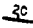
Qa	Alluvium
QTp	Paso Robles Formation
Tsm	Santa Margarita Formation
Tb	Basalt (hachured)
Tbs	Branch Canyon Sandstone
Tmw	Monterey Shale, Whiterock Bluff Shale Member
Tma	Monterey Shale, Saltos Shale Member
Tvp	Vaqueros Formation, Painted Rock Sandstone Member
Tvl	Vaqueros Formation, Soda Lake Shale Member
	Contact, dashed where inferred
	Fault
	Axis of anticline
	Axis of syncline
	Strike and dip of beds

Figure 2.2. Explanation of symbols used on geologic map.

Stratigraphic correlation of rock types contacting the fault has consistently shown right lateral movement since Cretaceous time. Surface features expressed at Wallace Creek enabled Sieh and Jahns (1984) to document slip rates averaging 1.33 inches per year for the last 3,700 years, and dextral slip ranging from 31.2 to 40.4 feet during the past three great earthquakes. Investigations of slip and creep rates along the San Andreas fault have led researchers to conclude that the Carrizo Plain contains part of a section of the fault which is locked. Strain of sufficient magnitude to cause a great earthquake ($M = 8$) is thought to be accumulating in this area.

An assemblage of three sedimentary sequences is located on the southwest side of the San Andreas fault. The first is a thick sequence of late Cretaceous and early Tertiary marine clastic sedimentary rocks. The sequence is not named. It is 30,000 feet in maximum thickness, comprised of interbedded arkosic sandstone, siltstone, clay shale, and granitic conglomerate. The conglomerate is 2,000 feet in maximum thickness, and is located at the base of the sequence.

The second sedimentary sequence is a Middle Tertiary (mostly Miocene) sedimentary sequence 10,000 feet in maximum thickness under the Carrizo Plain. These units are terrestrial at the base, marine in the upper part, and are

comprised of deposits from a granitic terrane that existed northeast of the San Andreas fault. The sequence represents a complete cycle of marine transgression, inundation, and regression. Basaltic intrusions and lava flows are present in both the marine and terrestrial units of this sequence.

The third sedimentary sequence is comprised of post-Miocene units. The units were deposited in a basin which extended through both the Salinas Valley and the Carrizo Plain between the Temblor Range uplift and the Santa Lucia-LaPanza-Sierra Madre Range uplift. The Quatal and Morales Formations comprise this Upper Tertiary sequence. They are nearly all terrestrial. The units overlie the Santa Margarita or Caliente Formations in the center of the Salinas basin, but unconformably cover all older formations on the flanks of the basin. This sequence is overlain by valley deposits late Pliocene to Recent, represented by the Paso Robles Formation and Recent alluvium deposited after the marine regression (Dibblee, 1973).

Tectonic Setting

A summary of the tectonic history is helpful in understanding the regional geology of the area. The following description summarizes the conclusions of recent work on the topic. For more detailed information, refer to Chipping (1988), Greene (1977), and Ross (1978).

Before Cretaceous time, the area which is now the western base of the Sierra Nevada was a plate margin at which the ocean floor was being subducted beneath the North American Plate. At the beginning of Cretaceous time, this margin shifted from the Sierra to the Coast Ranges, trapping a block of marine sediments and sea floor which would otherwise have been subducted. About 100 million years later, in Oligocene time, orogenic activity may have caused continental deposition, producing the red sands and gravels typical of alluvial fans. These red beds can be found in the Simmler Formation. The deposition may have been caused by orogenic activity, or by a major lowering of sea level. By Miocene time, the oceanic ridge producing the Pacific Plate had been subducted. Some volcanism ensued, and the new geometry produced the San Andreas right lateral faulting. Submarine basins then grew down from Santa Cruz and up from Santa Barbara. This was the period during which the shallow-water Vaqueros Formation was deposited. At the beginning of Miocene time, volcanic activity produced basalts in the Branch Canyon Sandstone. As the sea continued to regress, the littoral Santa Margarita Formation was deposited, followed by the terrigenous Quatal and Morales Formations (Chipping, 1972). This marine regression was contemporaneous with southeastern drainage patterns in early Pliocene time, as the uplift of the Santa Lucia and La Panza ranges

initiated deposition of the Paso Robles Formation. Near the end of the Pliocene, uplift in the Temblor Range and southwestward tilting of the Gabilan Mesa brought about the end of the period during which the Paso Robles Formation was deposited. This occurred because the southeast-flowing drainage was defeated, and the conditions for its capture by the modern Salinas River were created (Galehouse, 1967).

STRATIGRAPHY

Basement Complex

Ross (1977) refers to the area between the Red Hills-San Juan-Chimineas fault and the San Andreas fault as the Barrett Ridge slice of the southeastern block of the Salinian block. Most of the Mesozoic basement is relatively high-grade gneiss or ultrametamorphosed gneiss. Several oil wells drilled in this block encountered various kinds of gneiss, some amphibolite, and granitic rocks. Radiometric dating techniques suggest emplacement ages of 100-110 million years for the granitic rocks of the Salinian block.

Simmler Formation

The Simmler Formation is terrigenous, hard, red to greenish-gray, well-bedded sandstone, siltstone, and local conglomerate. The formation is 3,000 feet in thickness in the type section. No fossils are associated with the formation. The formation unconformably overlies both the Upper Cretaceous and Lower Tertiary marine sedimentary sequence and the crystalline basement complex, and is late Eocene to early Miocene. The average magnetic susceptibility of formation samples obtained is 53×10^{-6} cgs.

Vaqueros Formation

The Vaqueros Formation consists of two facies. One is mostly coarse-grained marine sandstone and the other is argillaceous sediments. Both facies were deposited under a transgressing sea. The Vaqueros is Late Oligocene to Early Miocene, ranging in thickness from 7,000 feet under the Carrizo Plain to less than 1,000 feet in the La Panza Range, which is located to the west.

Soda Lake Shale Member

This unit is dark gray, silty clay shale, claystone and siltstone, with a prominent chert bed in the middle of the section. The maximum thickness is 1,200 feet. The member's age is Saucian. The magnetic susceptibility of samples from this unit was near zero.

Painted Rock Sandstone Member

The Painted Rock Sandstone is fine-grained and fossiliferous in the upper part. It is medium- to coarse-grained, nearly white, and rarely fossiliferous in the lower part. The unit is 5,500 feet in maximum thickness, thick-bedded, and Early Miocene. It is overlain conformably by the Saltos Shale Member of the Monterey Shale. The unit overlies unconformably crystalline basement rocks in most locations. In some places it conformably overlies the Simmler Formation

and the Soda Lake Shale Member of the Vaqueros Formation. The member also contains reefs of shell debris locally, and exhibits bold outcrops. The average magnetic susceptibility of samples from the member is 18×10^{-6} cgs.

Monterey Shale

The Monterey Shale differs from the similar Monterey Formation exposed near Monterey. The latter lacks the distinctive shale of the Monterey Shale. This convention of nomenclature was adopted by Dibblee (1973), and is followed herein. The Monterey Shale is a Miocene, marine, mainly siliceous organic shale overlying the Vaqueros Formation. The unit is the most extensive Middle Tertiary sedimentary sequence in the Carrizo Plain. It was deposited in a period of maximum marine inundation.

Saltos Shale Member

At the type locality, this member of the Monterey Shale is comprised of gray shale and siltstone of Saucian age in the lower 1,000 feet. The upper 1,100 feet is soft fissile shale and hard, brittle siliceous shale interbedded with thin beds of dolomite. The upper section is Relizian. The member is locally intruded by a basaltic sill up to 75 feet in thickness. The member conformably overlies the Painted

Rock Sandstone. The magnetic susceptibility of samples from the Saltos Shale was near zero.

Whiterock Bluff Shale Member

This unit is a siliceous, fissile, brittle, thin-bedded shale containing locally abundant fish scales. The Whiterock Bluff Shale is 1,500 feet in maximum thickness. It is overlain by the Santa Margarita Formation gradationally, and is middle Miocene.

Branch Canyon Sandstone

The Branch Canyon Sandstone is a marine, coarse- to medium-grained, nearshore strandline deposit laid down between the offshore Monterey Shale to the southwest and the terrigenous Caliente Formation to the northeast. The sandstone is 3,200 feet in maximum thickness, and is overlain by the Santa Margarita Formation. It is thick-bedded, locally cross-stratified, light gray to yellow-gray, interbedded with greenish-gray siltstones. Magnetic susceptibility was near zero in samples measured.

Basalt

Dikes of basalt are abundant in the Vaqueros and Simmler Formations near Soda Lake. Sills of basalt are present in the Vaqueros Formation. Two basaltic flows are

known in the Branch Canyon Sandstone. The average magnetic susceptibility for basalt samples tested is 839×10^{-6} cgs.

Santa Margarita Formation

Overlying the Branch Canyon Sandstone is the Santa Margarita Formation. This unit is a white, friable, poorly-cemented, marine sandstone. It is a littoral facies produced by marine regression. The formation tongues eastward into nonmarine red beds and attains a maximum thickness of approximately 1,500 feet.

Paso Robles Formation

In the study area, the Paso Robles Formation unconformably overlies the Miocene sedimentary sequences. The formation is approximately 2,000 feet in thickness near the San Andreas fault, and thins southwestward. The Paso Robles Formation is comprised of pebble gravel, sand, and clay derived from the La Panza Range, from the Temblor Range, and from mountains west of the Salinas Valley. At the southern end of the Carrizo Plain, the formation contains detritus from the San Emigdio Mountains, located twenty miles to the southeast. The top of the formation is a surface of deposition preserved under a thin cover of alluvium. The formation is Pleistocene in the Carrizo Plain. There are no diagnostic fossils known for the formation in

the Carrizo Plain, but an outcrop two miles east of Atascadero did yield fossils indicating a Pleistocene age (Galehouse, 1967).

Surficial deposits

According to Chipping (1967), the Paso Robles Formation is difficult to discriminate from surficial deposits. In areas of the Carrizo Plain where the Paso Robles Formation is not deformed, the surficial deposits are conformable on the Paso Robles, and are mainly Holocene.

STRUCTURE

The Carrizo Plain is part of a basement thrust terrane consisting of large masses of Cretaceous, Eocene and younger rocks that have been pushed southwestward by northeast-dipping thrust faults (Chipping, 1987). The San Andreas fault borders the east side of the area. It is a major right-lateral fault with a zone of associated fault spurs and escarpments. A series of twelve north-south-striking faults along the southwest side of the site are on the northeastern limb of an anticline which is northeast of and parallel to the Big Spring thrust fault. The extent to which these faults continue under or through the valley sediments is important to this investigation. Although these are considered thrust or high-angle reverse faults, 2,000 feet of left-lateral offset is apparent along the westernmost fault (Figure 2.1).

METHODS, RESULTS, AND INTERPRETATIONS

This investigation utilized magnetics, borehole geophysics, piezometric levels, and drillers' logs to analyze the area's hydrogeology. A major part of the field work was a magnetic survey to obtain information concerning bedrock depths and faulting in the area. Conclusions of the study were based on interpretations of (1) magnetics measurements, (2) electric logs, (3) thermal logs, (4) measurements of piezometric levels, and (5) other related data, such as existing water and oil well logs, geologic maps and rainfall data. Two computer programs were utilized for data reduction. Magnetic data were tabulated with the Magpac 4.1.3 program for magnetic analysis, manufactured by Geometrics, Inc. Both magnetic and temperature data were plotted with Grapher 1.75 from Golden Software, Inc. The following discussion presents for each method a summary of the geophysical principle applied, a description of the results obtained, and an interpretation of those results.

Magnetic method

The area was investigated magnetically by measuring the total magnetic intensity in order to locate significant anomalies (distortions of the local field). Distortions of the field by rocks containing contrasting amounts of

magnetic material produce anomalies, the character of which is determined by the geometry, orientation and magnetic properties of the rocks, and the direction and intensity of the Earth's magnetic field. Most rocks contain some magnetic materials (usually magnetite), but sedimentary rocks usually contain smaller amounts of these materials, and thus are not discernible by magnetic sensing. Igneous and metamorphic rocks usually contain more magnetic minerals. They are therefore the most common cause of magnetic anomalies in sedimentary basins (Zohdy and others, 1984). Anomalies several hundred gammas in size may be interpreted as changes in lithology. Ten to one hundred-gamma anomalies may be interpreted as changes in basement structure (Breiner, 1973).

Magnetic investigation

For this investigation, a model G856A proton-precession magnetometer manufactured by Geometrics, Inc. was used. Daily field data were stored in the magnetometer memory for later transfer to computer memory discs. Measurements were made along eight lines, varying in length from 0.4 miles to 2.5 miles, at stations 100 feet apart (Figure 3, Table 1). The lines were oriented perpendicular to previously mapped geologic structures to the extent that surface access made such positioning practical. Base station measurements were

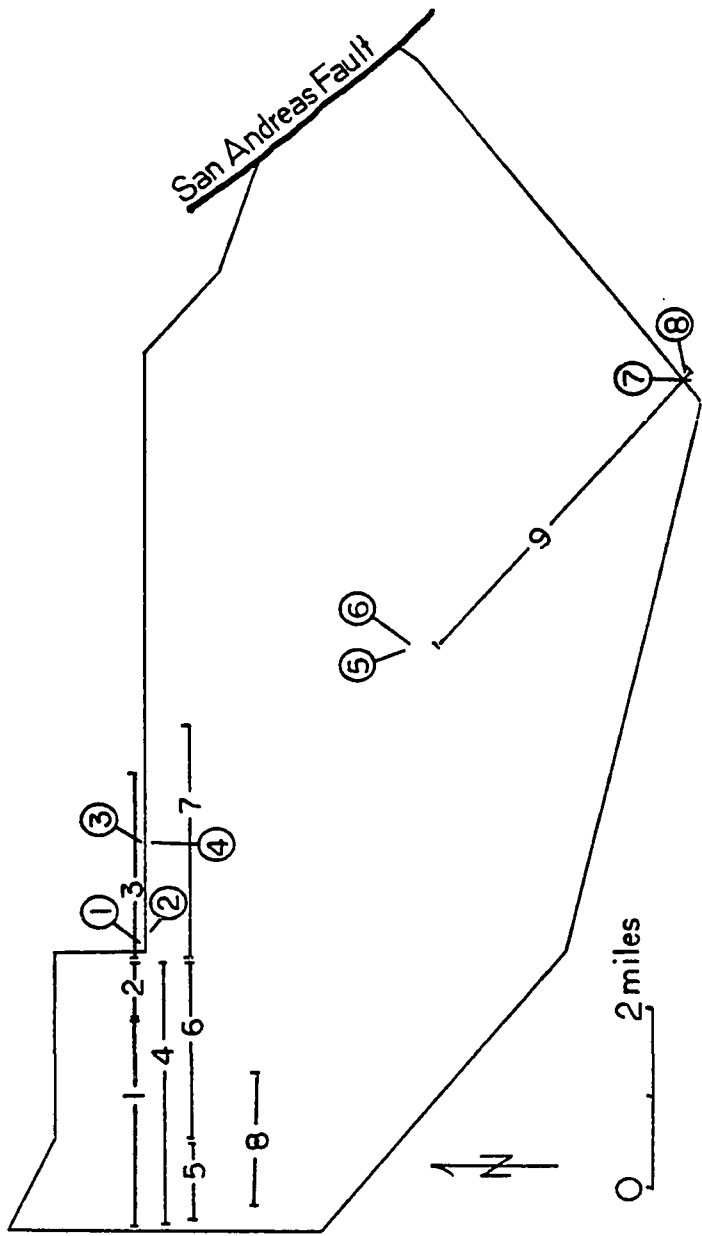


Figure 3. Map showing the location of magnetometer survey lines and wells.
 Circled number indicates well.

Table 1. Nine linear magnetometer surveys, 15.9 mi. in total length. Measurement intervals are 100 feet.

<u>Line No.</u>	<u>Stations</u>	<u>Length (mi.)</u>
1	282-410	2.4
2	411-444	0.6
3	451-555	2.0
5	6-54	0.9
6	55-163	2.0
7	172-304	2.5
8	290-310	1.5
9	3-216	4.0

performed at one-half to two hour intervals. Variations in base station measurements were less than seventeen gammas for any line. Diurnal corrections were completed. Data supplied for the United States Geological Survey magnetic observatory in Fresno, California showed that there were no variations greater than fifteen gammas during periods of the field investigation.

A magnetic contour map and profiles of magnetic intensity along measured lines were completed and used for the interpretations. The contour map (Figure 4) was produced by selecting measurements from the linear survey which were taken nearest the section corners. Where there were no

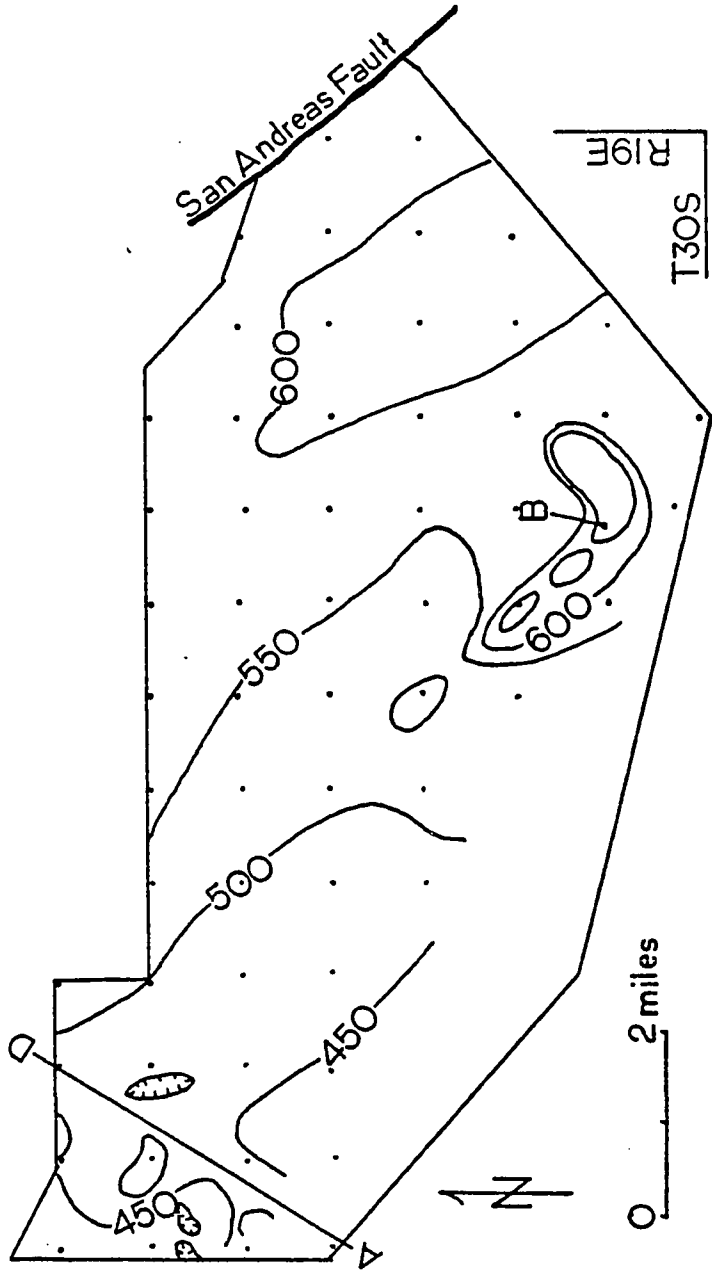


Figure 4. Contour map of total magnetic intensity. Magnitude at B is 50,450 gammas. A fault location is postulated at AD, where northwest-trending lines are truncated. Units: gammas +49,000. Contour interval: 50 gammas. Dots represent data points.

nearby line measurements, additional measurements were taken to complete a one-mile-square grid. The measurements were taken over a period of two months.

Several magnetic features are evident on the contour map and on the magnetic profiles. The level of magnetic intensity increases from approximately 48,400 gammas on the southwest border to approximately 48,600 gammas on the northeast border. This regional trend is shown in part with the magnetic profile of line number seven (Figure 5.7). The easterly rate of increase for this line is consistent, at approximately 44 gammas per mile. Isogams trend northwest, parallel to the San Andreas fault. Exceptions to this regional pattern are the anomalies toward the northwest and southwest corners. The northwestern anomaly appears to truncate the northwesterly trend of the isogams at the northeast-trending line A-D (Figure 4). The southwestern anomaly (B on Figure 4) is a magnetic peak of approximately 850 gammas. Line number nine was surveyed approximately 1000 feet northeast of the peak. The profile located at this line shows the anomaly as a double peak approximately 360 gammas in amplitude and 4,600 feet in width (Figure 5.1).

Interpretation of magnetics

The increase of 200 gammas in magnetic intensity from the southwest boundary of the area of investigation to the

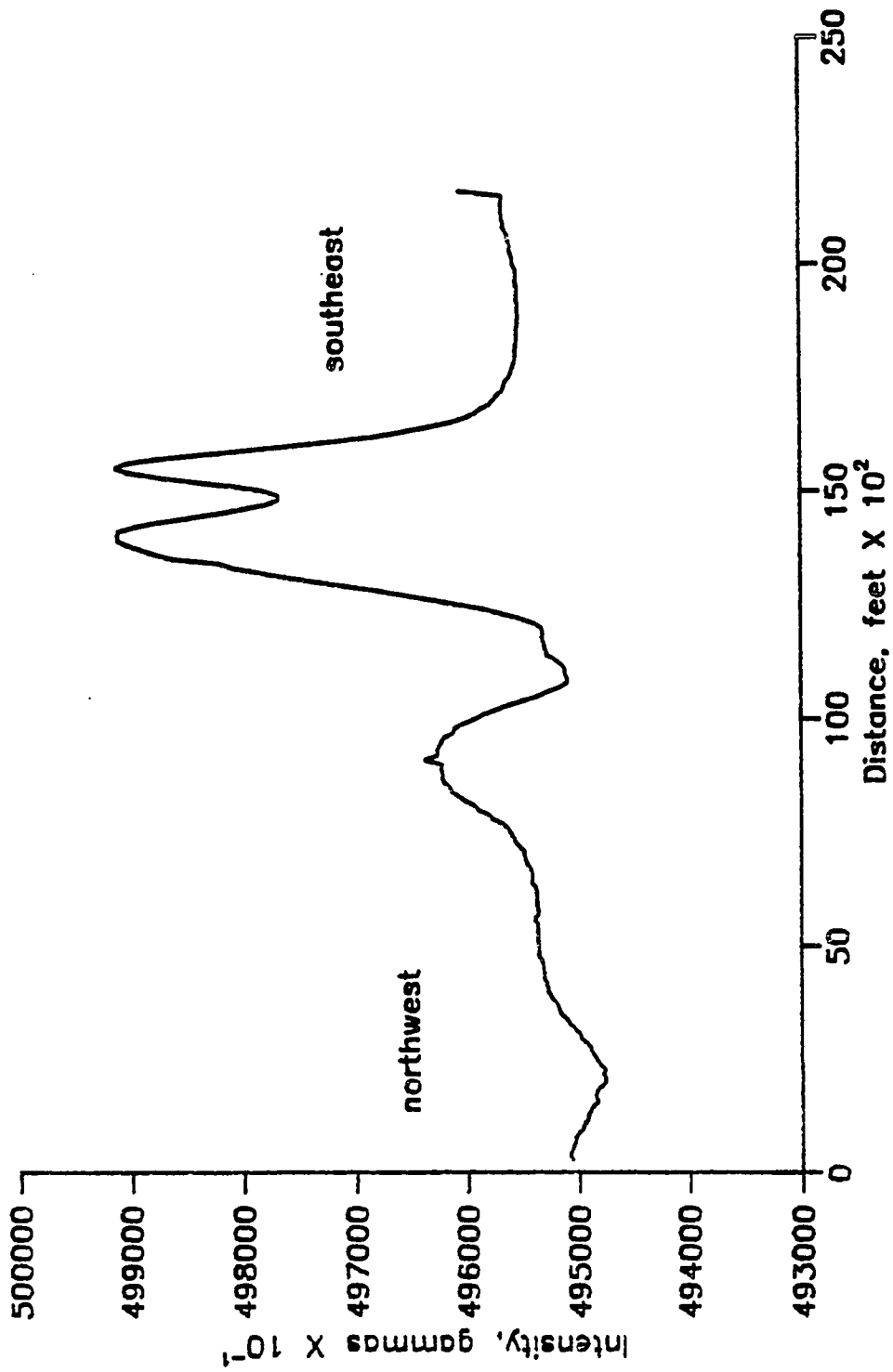


Figure 5.1. Total magnetic intensity of line 9. A basaltic dike is postulated as the cause of the southeastern anomaly.

San Andreas fault may be caused by an increase in magnetic susceptibility of either the crystalline basement rocks, or the overlying wedge of sedimentary deposits. The magnetic susceptibility of sedimentary rocks sampled in the area is low (Table 2). However, there may be beds within the sedimentary units which have greater levels of magnetic susceptibility and which thicken near the San Andreas fault, where basement rocks are deepest. Right-lateral offset of the San Andreas fault may have moved these beds from their source. If there are sedimentary beds with greater magnetic susceptibility, their source may be the San Emigdio and Tehachapi mountains to the south. These mountains are highly mineralized and may have supplied magnetic sediment. There are no borehole magnetometer data available to support or contravene this hypothesis, nor has an outcrop of sedimentary rocks with high magnetic susceptibility been reported in the area.

The eastward increase cannot be explained by a declining easterly depth to bedrock, because Dibblee (1965) has described the general topography of the surface of the basement rocks as dipping to the northeast. This description is consistent with oil well logs in the area. The magnitude of change in magnetic intensity of hundreds rather than tens of gammas, suggests a lithologic rather than a structural change. For these reasons, the hypothesis that the increase

in magnetic intensity is caused by a decrease in depth to basement rock was rejected.

Table 2. Samples tested for magnetic susceptibility with a Soiltest MS-3 magnetic susceptibility bridge.

<u>Sample</u>	<u>Description</u>	<u>Magnetic Susceptibility</u> <u>(10⁻⁶ cgs)</u>
1	Painted Rock Sandstone	18
2	"	18
3	"	18
4	Soda Lake Shale	0
5	"	0
6	"	179
7	Simmler Fm.	264
8	"	0
10	"	0
11	"	0
13	"	0
14	Branch Canyon Sandstone	0
15	"	0
16	"	0
19	"	0
17	Basalt	928
18	"	750

The eastward increase in magnetic intensity is probably due to an eastward increase in magnetic susceptibility of the basement rock. The basement rock is considered part of the Salinian block, a granitic basement terrane which contains a positive aeromagnetic anomaly 100 miles to the north (Ross, 1978). Granitic rocks do not crop out in the study area, nor were borehole samples available for this investigation. In the Monterey Bay area, granitic basement rock was found to have a magnetic susceptibility of 761.5×10^{-6} cgs (Grasty, 1988). This is a marked contrast to the average magnetic susceptibility of 37×10^{-6} cgs found for sedimentary rocks in the study area. The anomalous magnetic maximum in the southeast quarter of section 29 is shown in the profile of line number nine and in the magnetic contour plot (Figures 4 and 5.1). The 360-gamma amplitude of the maximum indicates a change in lithology rather than basement structural deformation. Using graphic methods of analysis, the anomaly width of 4,600 feet indicates a depth to the top surface of the anomalous body of 1500 to 4600 feet (Breiner, 1973; Nettleton, 1976). Several observations led to the conclusion that this anomaly was caused by a basaltic dike. The magnetic susceptibility of basalt is an order of magnitude greater than that of any other rocks tested. Dibblee (1973) states that basaltic dikes are locally abundant in the Vaqueros and Simmler Formations near Soda

Lake. The curve produced by modelling a basaltic dike resembles that observed for the line number nine profile (Figure 5.1).

The curve for comparison was produced by computer modelling of a dike striking perpendicular to line number nine (Figure 5.2). The magnetic susceptibility of the dike rock was assumed at 900×10^{-6} cgs, which was the value for a basalt sample tested. The dike model was prismatic in shape, 1,000 feet in width at the top surface, 4,000 feet in length, and ten feet in depth to the top surface, and infinitely deep to the bottom surface. The program used was Magpac 4.1.3. Although the modelled curve varies in shape from the observed curve, it is similar in amplitude and width. Variations in shape between the two curves may be caused by basement topography more complex than the simple prismatic shapes to which the model is limited.

The anomaly at AD, located on the magnetic intensity contour map (Figure 4) was interpreted as an extension of faults mapped by Dibblee (Figure 2.1). Several facts support that interpretation. The anomaly and the fault traces both trend northeastward. The 1700-foot left-lateral component of movement of the westernmost fault and its truncation at the alluvium contact indicate that the fault extends through basement rocks concealed by valley sediments. Two points of inflection on the profile of line number eight (Figure 5.3)

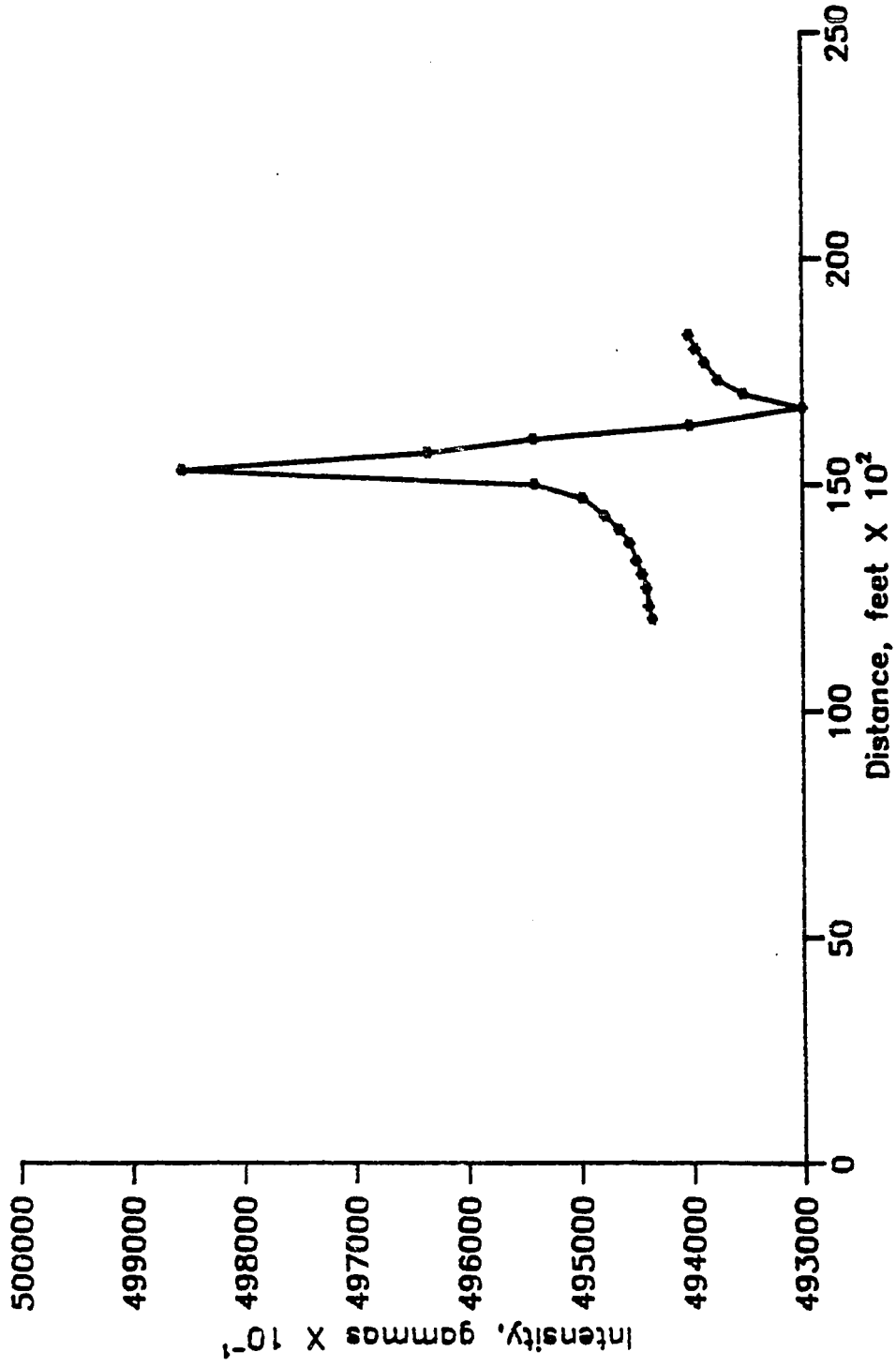


Figure 5.2. Computer model of the magnetic anomaly caused by a dike with magnetic susceptibility of 9×10^{-4} cgs, striking perpendicular to line 9.

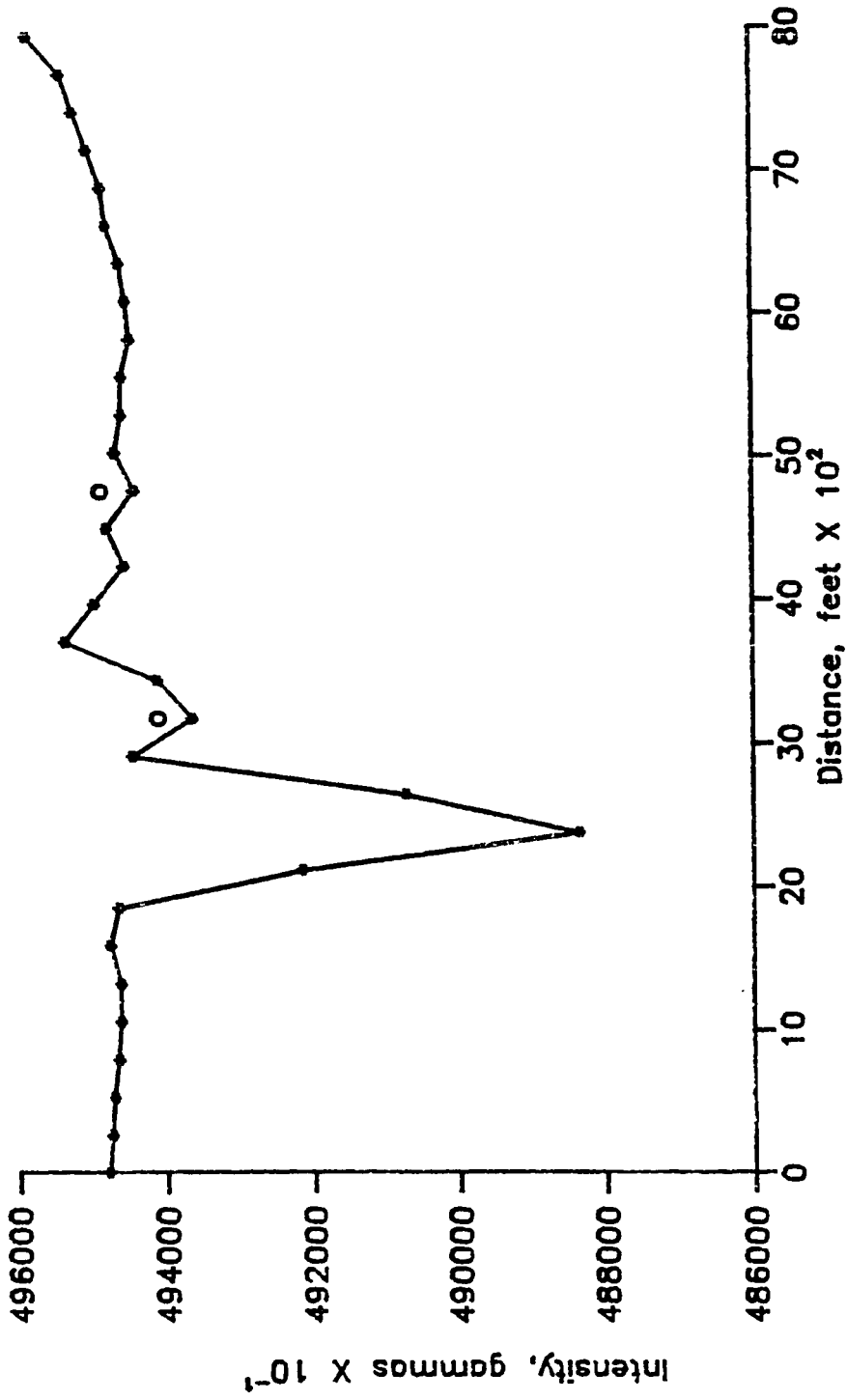


Figure 5.3. Total magnetic intensity of line 8. Inflection points of the curve are located under the circle.

occur at the fault locations. Lines one, two, five, six, and four are oriented perpendicular to the fault strike. The profiles of these lines (Figures 5.8, 5.5, 5.6, 5.4) contain points of inflection which lie in a linear zone projected from the fault traces mapped by Dibblee (Figure 2.1).

Variations in magnetic intensity (excluding noise) along these profiles range from 40 gammas for line number six to 100 gammas for line number four. This range of variation indicates the presence of a geologic structure such as a fault or a fold.

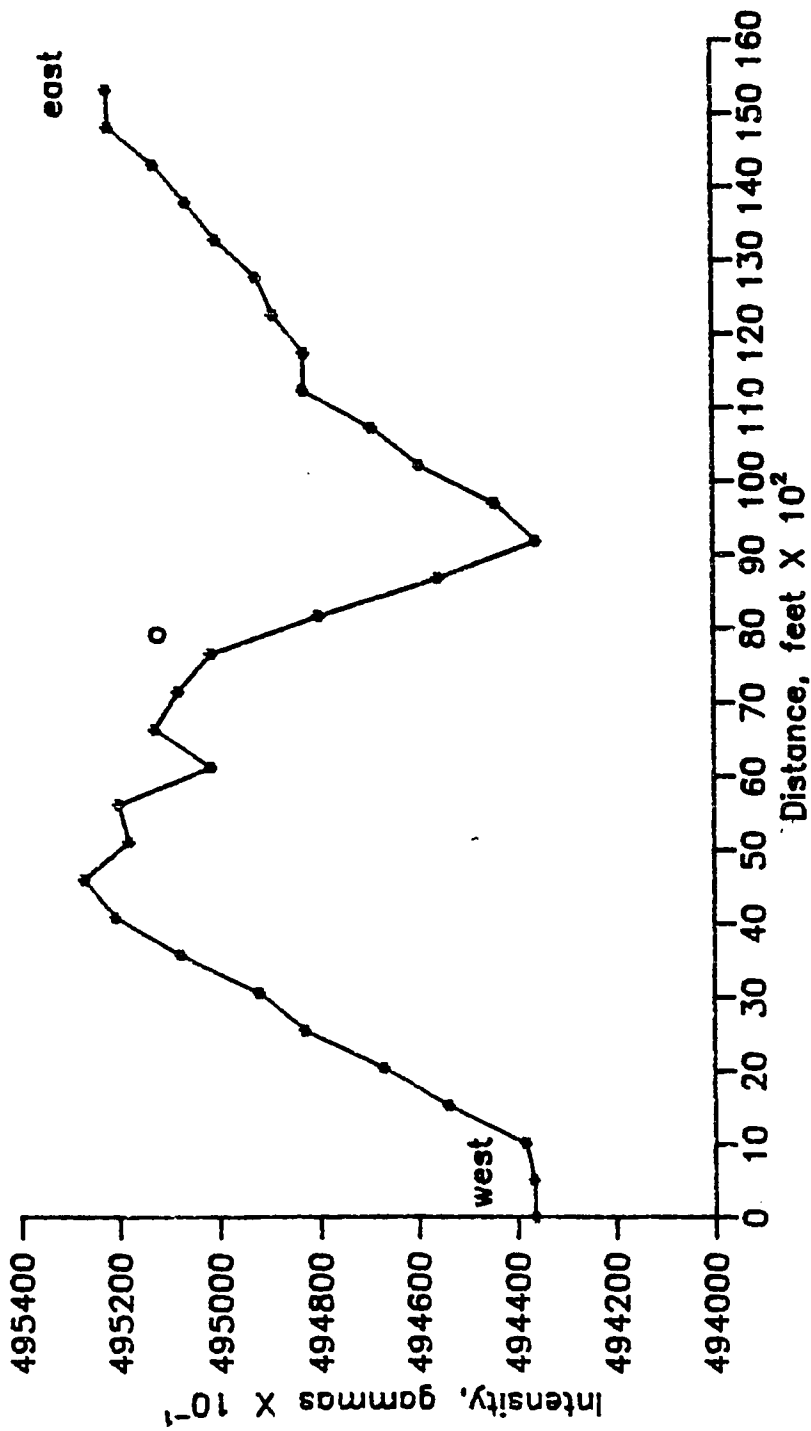


Figure 5.4. Total magnetic intensity of line 4. Inflection point of the curve is located under circle.

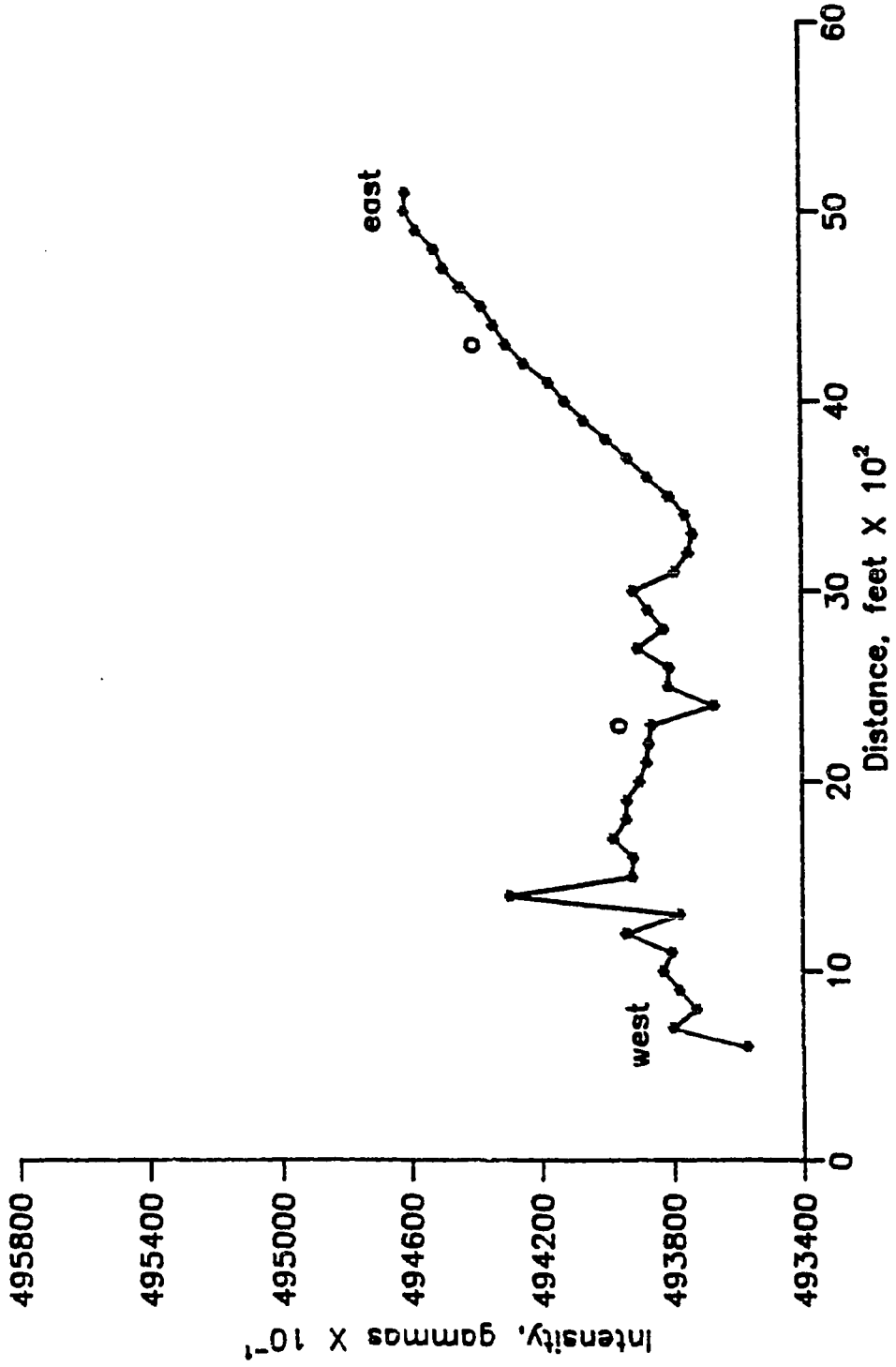


Figure 5.5. Total magnetic intensity of line 5. Inflection points are located under circle.

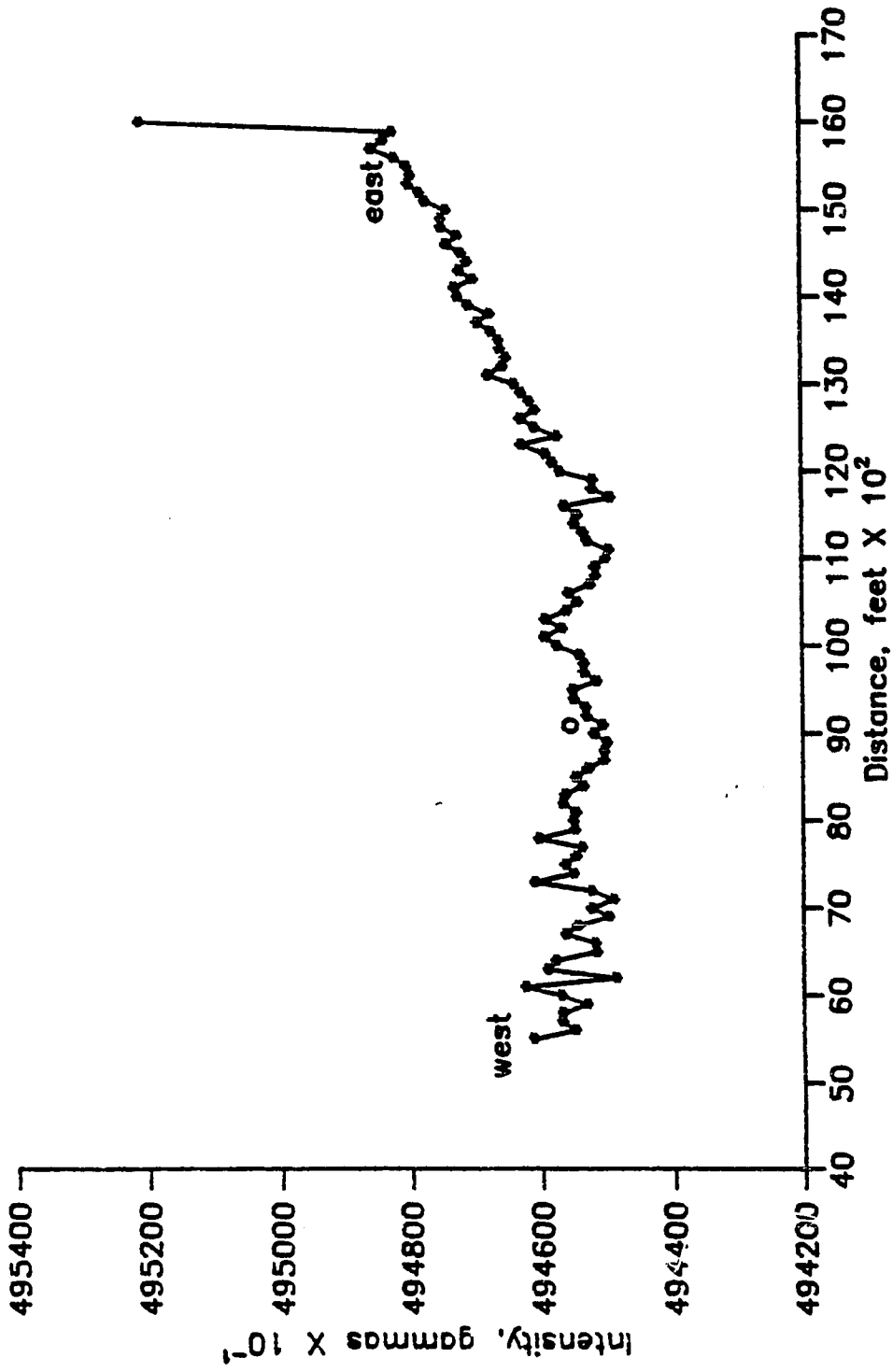


Figure 5.6. Total magnetic intensity of line 6. Inflection point of the curve is located under circle.

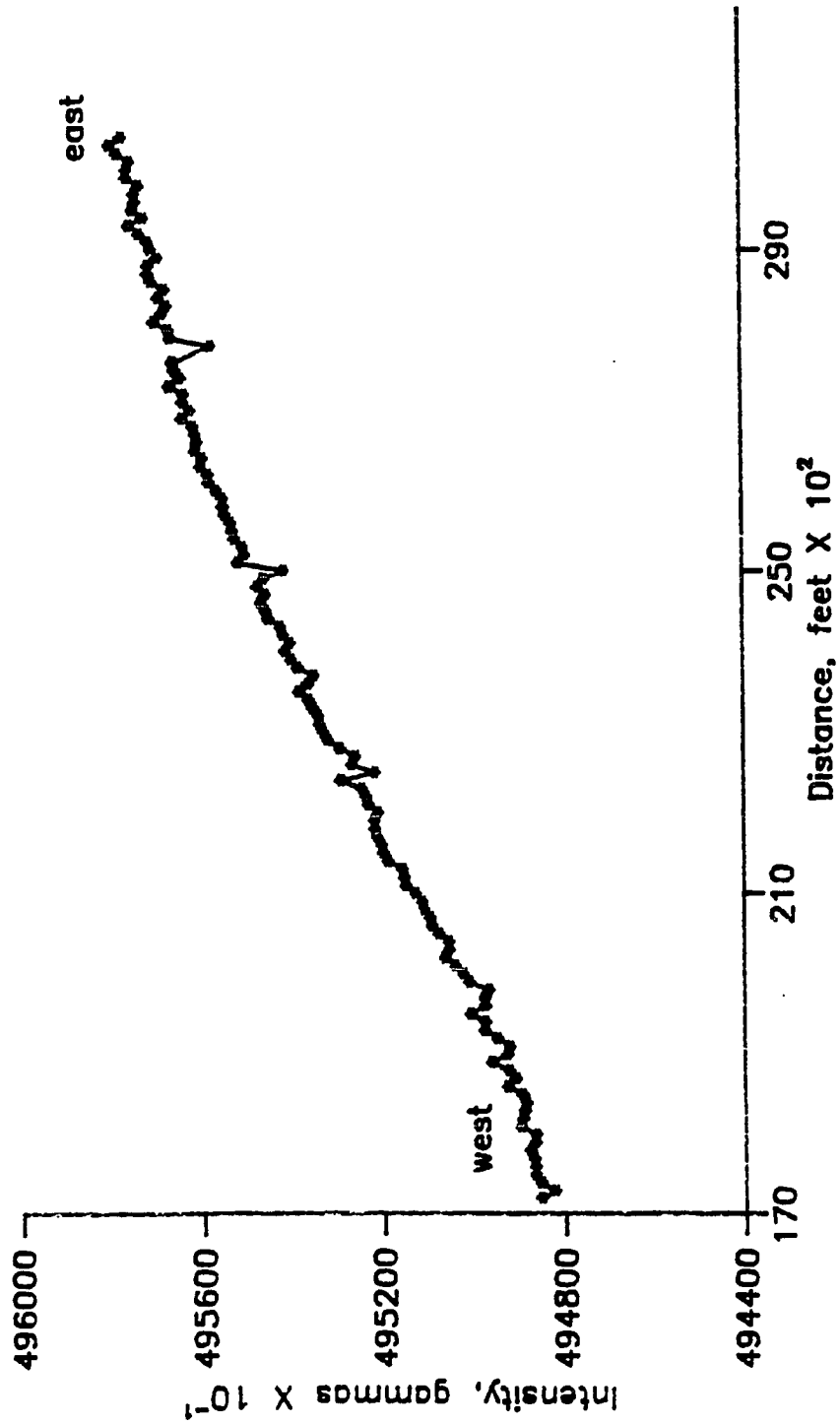


Figure 5.7. Total magnetic intensity of line 7, showing an increase of 100 gammas from west to east.

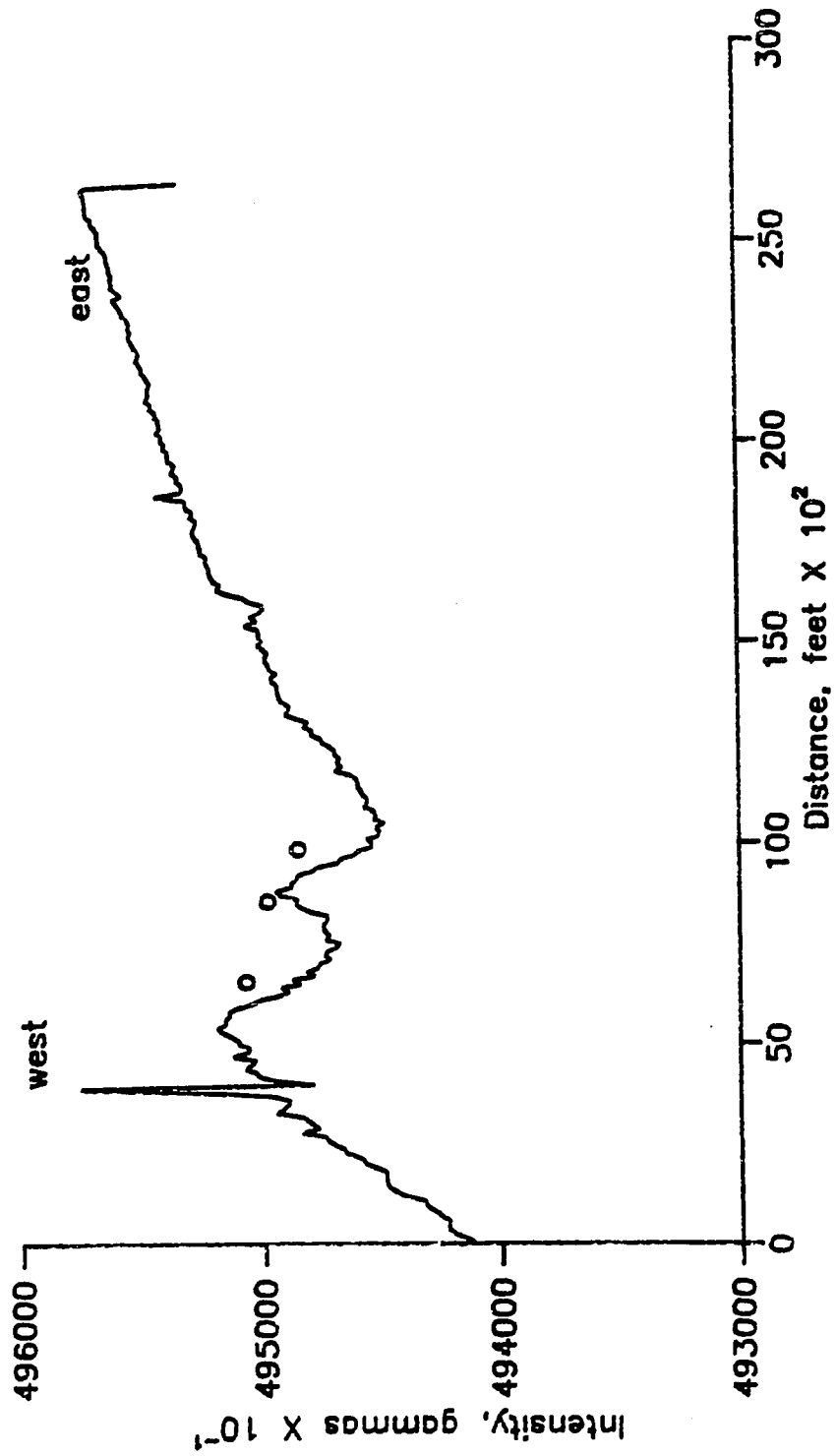


Figure 5.8. Total magnetic intensity of lines 1, 2, and 3. Inflection points of the curve are located under circle. Measurement increment: 100 feet.

Thermal logging method

A thermal logging investigation of the hydrogeology was completed, and this supplied important supporting evidence for the analysis. The application of thermal logging to hydrogeologic investigations is dependent on an understanding of the mechanisms controlling heat emanating from the Earth's interior. Temperatures in the Earth's crust increase at an average rate of 1 to 1.5°F per 100 feet of depth (Keys, 1971). The gradient varies depending on local heat flow and conductivity of both the rocks and the water. Heat conductivity in an aquifer varies with ground water movement and convection. The heat conductivity of water in units of 10^{-3} calories per second-inch-degree fahrenheit is 2.0. By comparison, the value for bedrock is a range of 7 to 16, and for unconsolidated sediments, 0.6 to 1.3. Table 3 lists thermal conductivities of other geologic materials. An increase in permeability and an attendant decrease in grain-to-grain contact facilitate heat flow in unconsolidated sediments. The temperature increase per unit heat flow is less in permeable, saturated materials than in consolidated materials. Because of these geophysical properties, changes in lithology or permeability influence borehole logs of temperature.

Table 3. Thermal conductivities of selected geologic materials (adapted from Birman, 1969).

<u>Category</u>	<u>Representative Material</u>	<u>Thermal Conductivity</u> <u>10^{-3} cal/in sec $^{\circ}$F</u>
Bedrock	Igneous rocks	7-11
	Consolidated sediment	4-16
Unconsolidated sediment	Sand	0.8-1.3
	Silt, loam	0.6-1.3
	Clay	0.4-0.8
	Water 32 $^{\circ}$ F; 1 atm.	2.0

To obtain accurate measurements of thermal gradients in wells, the fluid temperature must be in equilibrium with the casing and the formations penetrated, and there must be no vertical circulation in or adjacent the bore. Since some vertical flow is likely in the filter pack of the annular space, it is probable that thin layers will not be resolved by temperature logs. This does not preclude the usefulness of the method in locating water-bearing formations. The background geothermal gradient is distorted near the surface, where diurnal and annual surface temperature

variations effect soil temperatures to a maximum of fifty feet in depth (Lovering and Goode, 1963).

Five selected wells were analyzed by thermal logging (Figure 3, Table 4). These wells were selected to provide representation for the entire study area, including a range of water quality from the best to the worst for the area. Resistivity, SP, and drillers' logs were available for most of the wells. This allowed the testing of hypotheses with independent sources of data. None of the wells had been recently pumped and therefore the temperature of the casing, pumping assembly and borehole water were in equilibrium with the rocks. The wells analyzed were the deepest in the area for which a variety of information was available. The greater depth provided access to more rocks below the zone of surface temperature-induced anomalies. The northern wells are located in the thinner part of the wedge of valley sediments eight miles westward from the San Andreas fault, at the northern extent of the Caliente Range. The southern wells are five miles westward from the San Andreas fault, within one-half mile of Soda Lake.

Thermal logging investigation

Thermal logging measurements were made using an Omega model 450-ATH digital thermometer with an Omega series 400 thermistor input. The stated resolution was 0.1°F. The

thermistor was attached to the thermometer with a connector at the end of a spool-mounted cable. Logs were recorded with the first pass down the borehole to insure minimum disturbance of the water column. Measurements were made at ten-foot intervals, after allowing the thermistor time to equilibrate at each station.

Table 4. Location of wells cited in this investigation as designated by the California Department of Water Resources identification system.

<u>Well number</u>	<u>DWR identification number</u>
1	29/18 34N2
2	30/18 3D2
3	29/18 35N1
4	30/18 2D2
5	30/19 18N1
6	30/19 18P1
7	30/19 34N1
8	30/18 34N2

The log thus produced for well number three (Figure 6.1) shows a cooling descent pattern near the surface,

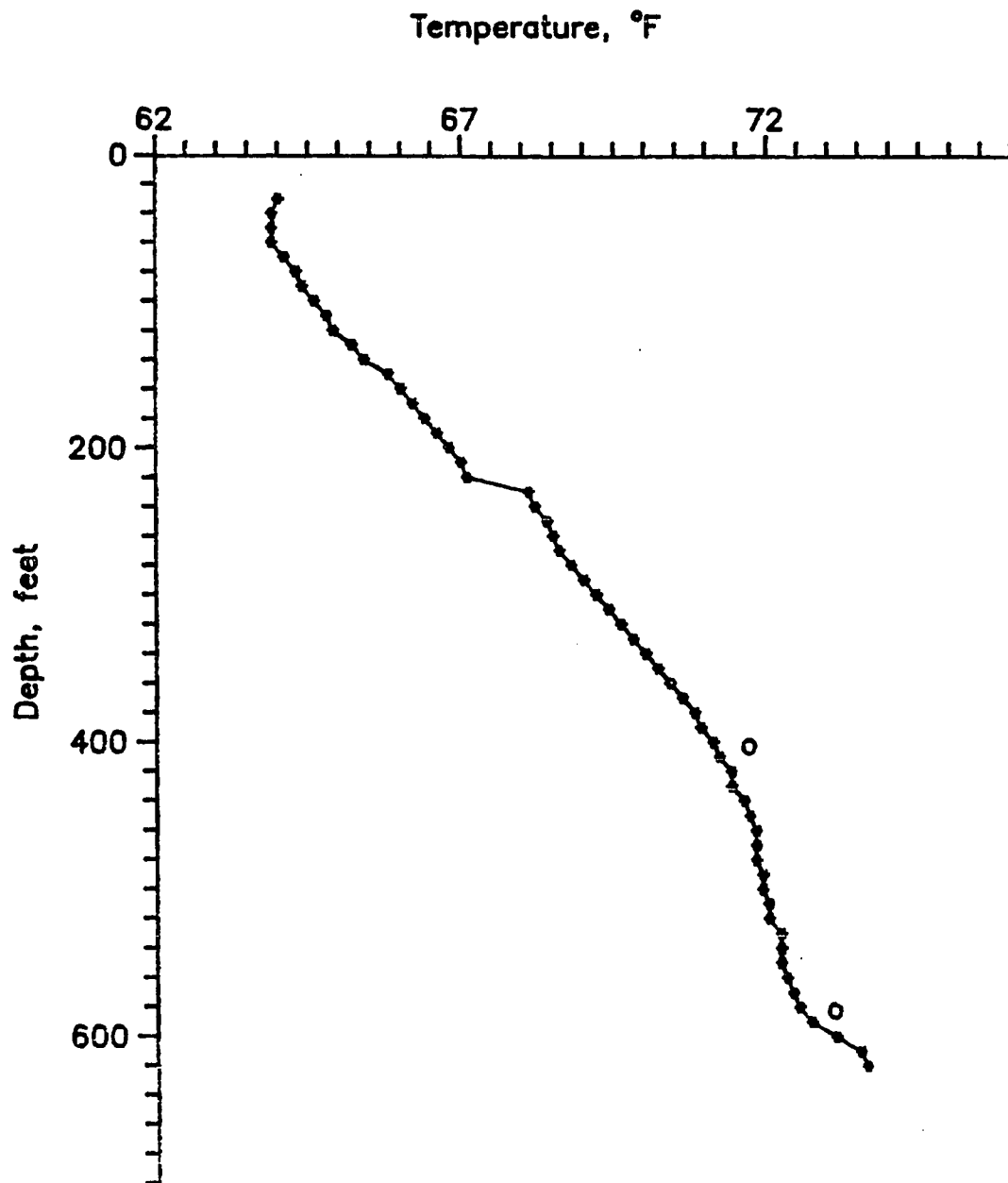


Figure 6.1. Water column temperature of well number 3. Depth of change of thermal gradient is located at circle. Date: 7/31/89.

typical of most of the wells measured. The warming effect of July and August surface temperatures is the predominant thermal gradient to a depth of approximately 60 feet. The two depth intervals 60 to 400 feet and 580 to 615 feet have gradients of 1.9°F and 5°F per 100 feet, respectively, indicating zones of high thermal conductivity. The gradient of the 400-foot to 580-foot interval is an order of magnitude less, at 0.3°F per 100 feet.

The thermal log of well number five (Figure 6.2) indicates that formations between 200 feet and 500 feet in depth are less heat-conductive than those above and below that interval. The 70-foot to 170-foot interval thermal gradient is 0.9°F per 100 feet of depth and the 500-foot to 580-foot interval thermal gradient is 1.5°F per 100 feet of depth. The gradient of the intervening interval of depth is 2.2°F per 100 feet of depth.

The thermal log of well number four (Figure 6.3) displays the air temperature-induced reverse surface gradient to a maximum depth of 60 feet. The thermal gradients for the 60- to 100-foot interval and the 180- to 257-foot interval are 1°F per 100 feet and 1.4°F per 100 feet, respectively. The intervening 100- to 180-foot interval has a relatively greater thermal gradient of 2.7°F per 100 feet of depth.

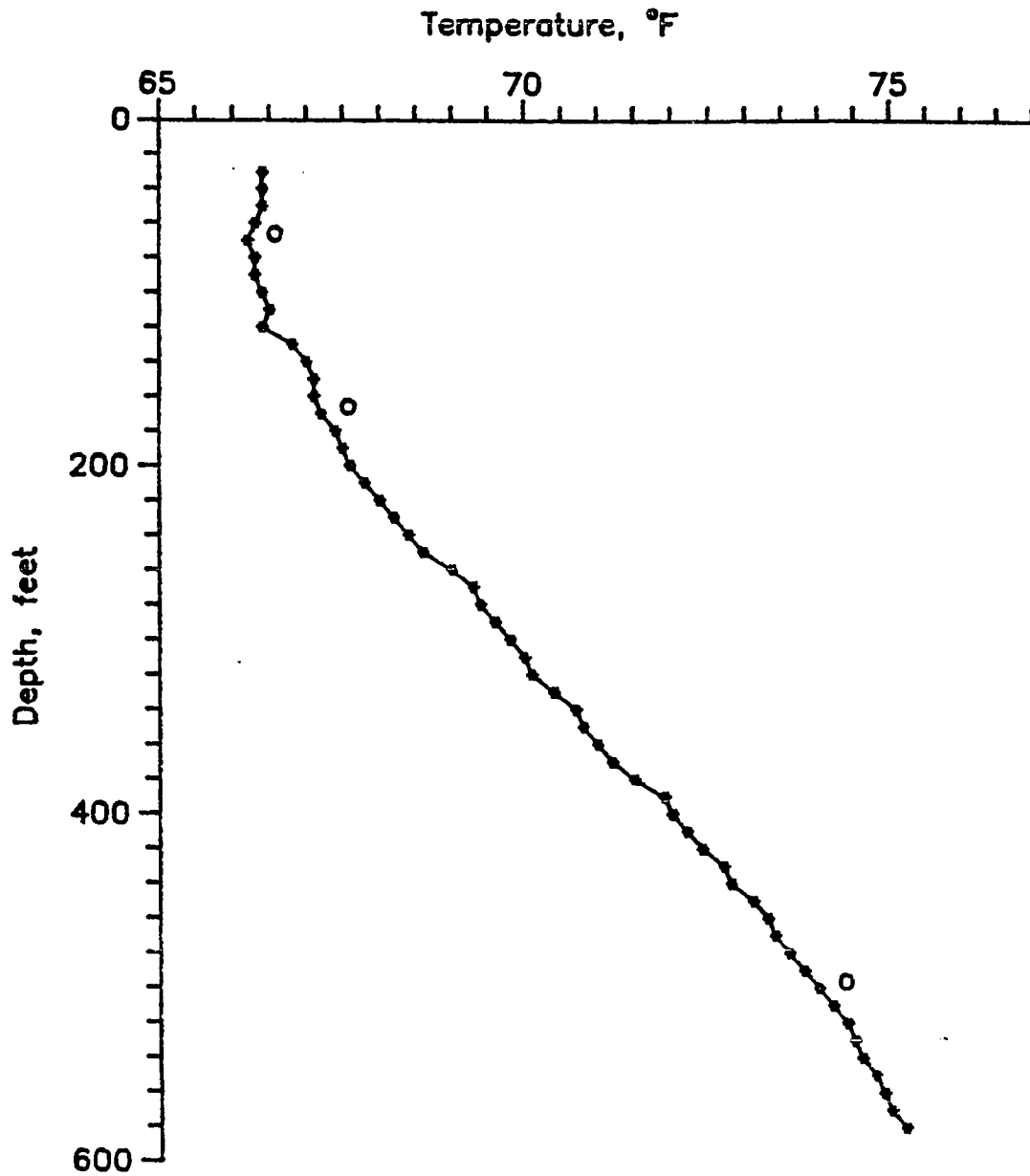


Figure 6.2. Water column temperature of well number 5. Depth of change of thermal gradient is located at circle. Date: 7/29/89.

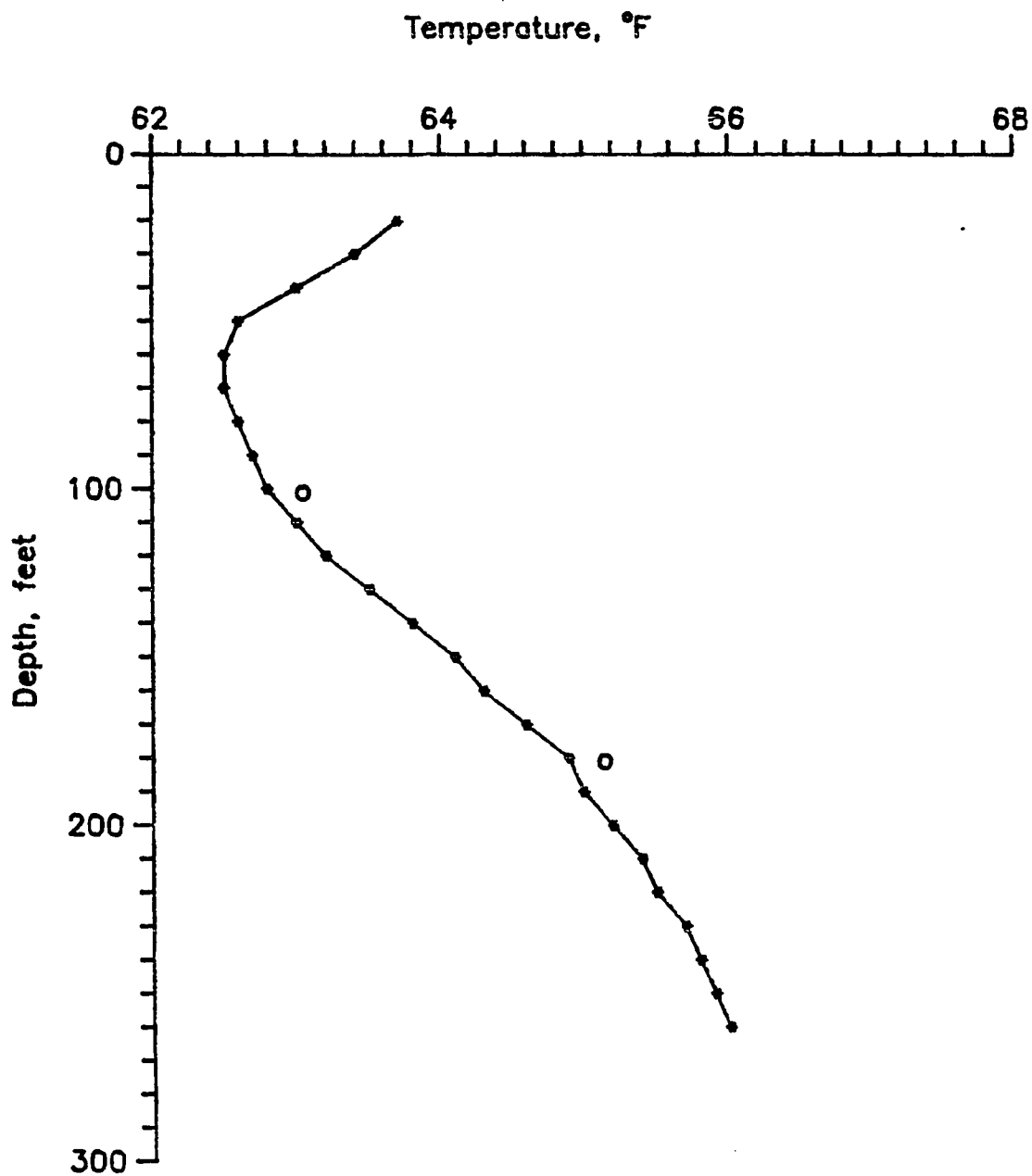


Figure 6.3. Water column temperature of well number 4. Depth of change of thermal gradient is located at circle. Date: 7/28/89.

The thermal log of well number seven (Figure 6.4) slopes consistently at 1.75°F per 100 feet in depth. The gradient is maintained throughout the logged depth below the reverse surface gradient, except for the anomalous increase in temperature at 850 feet in depth. The thermal gradient of well number eight (Figure 6.5) is 0.7°F per 100 feet in depth from 60 feet to 135 feet. From 135 feet to 580 feet in depth, thermal gradients range from 1.6°F to 7.1°F per 100 feet. Below 580 feet, the gradient is 0.4°F per 100 feet.

The thermal gradient of well number two (Figure 6.6) does not exceed approximately 1°F per 100 feet in depth. This value is represented by the slope of the curve between 120 feet and 200 feet in depth. Relative to the gradient of measured formations in the remainder of the borehole, this interval of depth is less conductive thermally. Thus the graph indicates that the primary water producing zones of this well are not between the 120-foot and 280-foot levels of depth. Contrary to the pattern of all other thermal logs in this investigation, the initial slope of the curve at zero depth is one of increasing rather than decreasing temperature with increasing depth. This is because the measurement was performed in February, when air temperatures were lower than water temperatures.

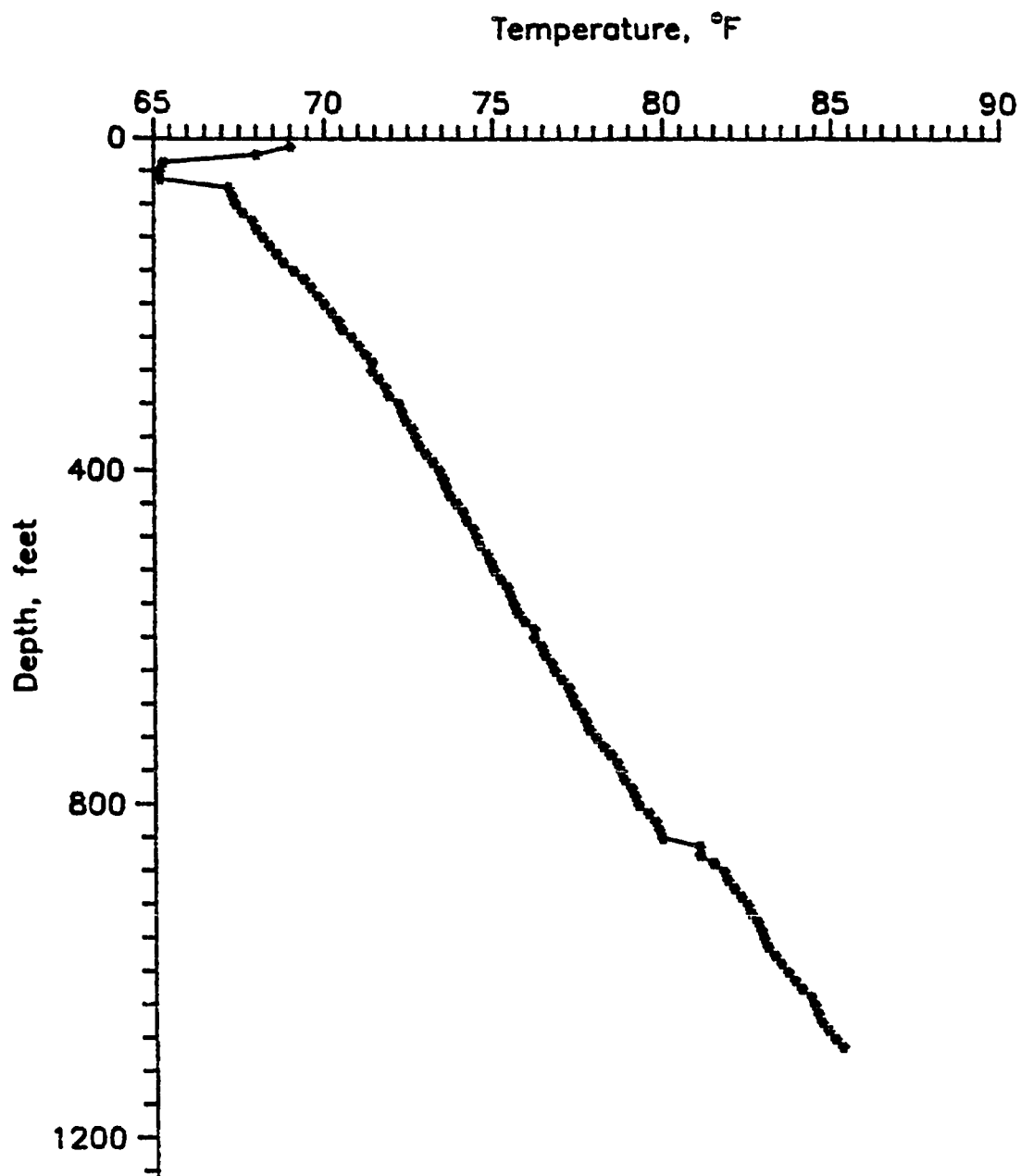


Figure 6.4. Water column temperature of well number 7.
Depth logged: 1080 feet. Date: 7/28/89.

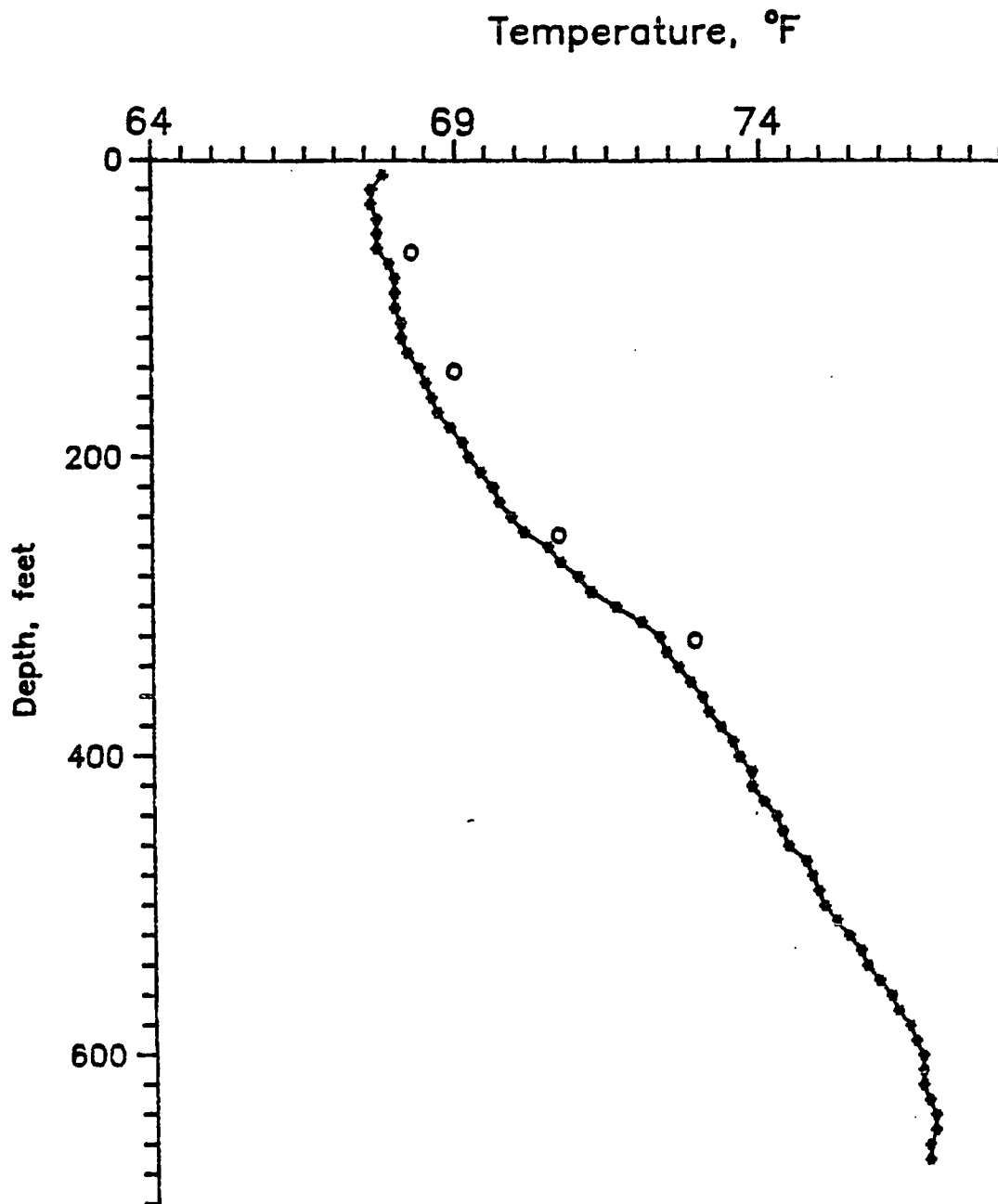


Figure 6.5. Water column temperature of well number 8. Depth of change of thermal gradient is located at circle. Date: 7/29/89.

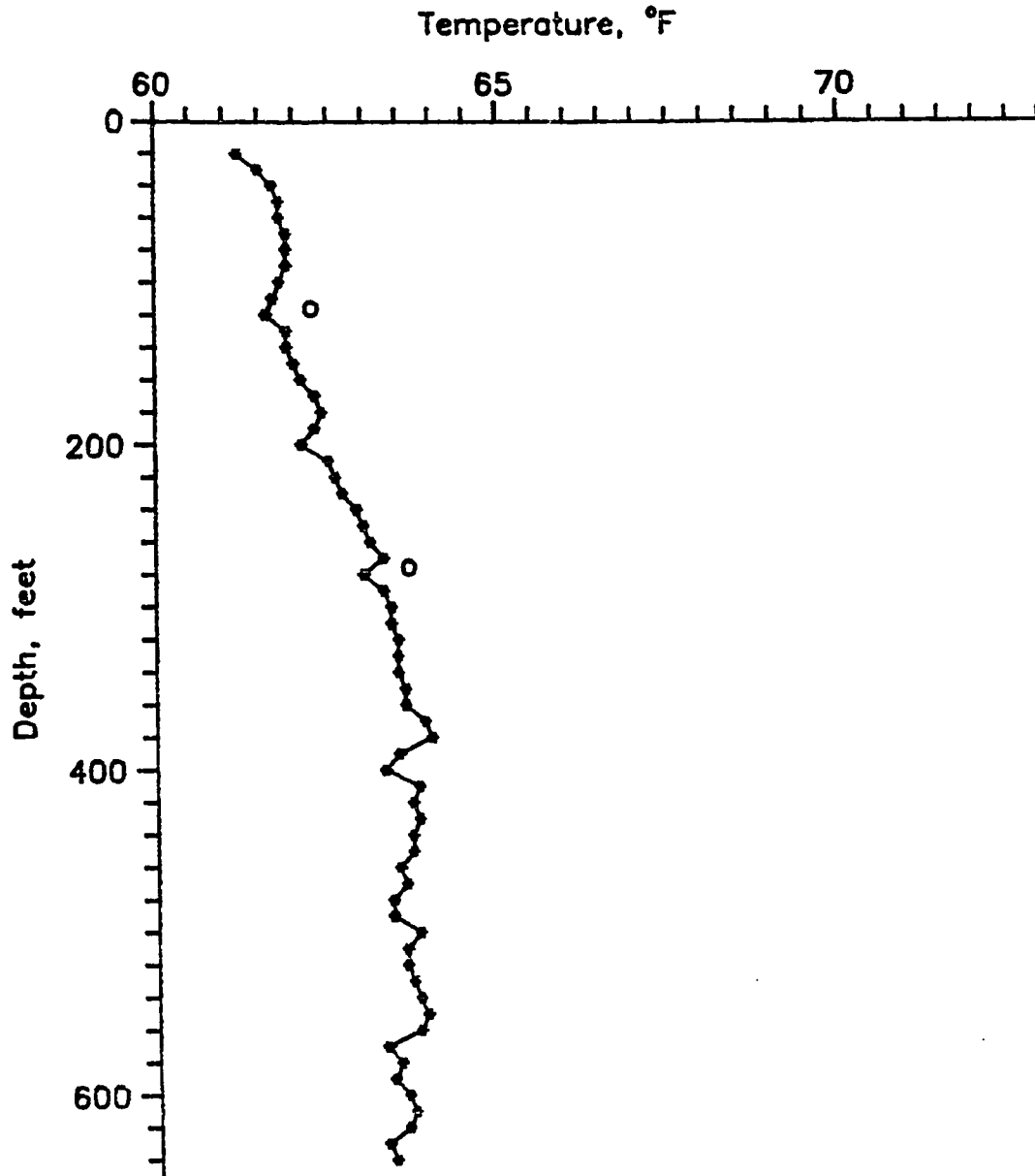


Figure 6.6. Water column temperature of well number 2. The curve slopes approximately 1°F per 100 feet between circles. Date: 2/8/90.

Interpretation of thermal logs

Several general and specific geological interpretations were made from the thermal well log analysis. The thermal log interpretation required several reasonable assumptions regarding geological, hydrological, and thermal factors. It was assumed in this investigation that the thermal source is deep within the earth. Local geothermal sources are unknown. It was also assumed that seasonal effects of groundwater movement from recharge areas to discharge areas would not change the conclusions of the investigation, because measurements were made vertically and were analyzed by comparison of depth-varying temperatures at each well.

Some characteristics of the curves are not related to aquifer properties. For well number three and well number five, the cause of the abrupt shift in the curves to the right at 270 feet and 840 feet in depth, respectively, is undeterminable at the present time. The sonde may have become temporarily entangled during descent, lowering less than the ten-foot interval measured at the surface. It may then have dislodged, falling more than the ten-foot interval before the subsequent measurement. There may also be a geological cause for the anomaly.

For all of the curves, the surface air temperature influence is assumed to penetrate to approximately 60 feet

in depth. The apparent low thermal gradient below 580 feet in depth of well number eight may be caused by a casing obstruction which arrested penetration of the sonde. Pump test reports indicate that damage to the well occurred during testing.

Although there was no lithologic or geophysical log available for correlation with the thermal log for well number four, the changes in the thermal gradient indicate that some sand or gravel interbeds are located from 60 feet to 100 feet in depth and from 180 feet in depth to bottom. The interbeds are probably of limited extent, as indicated by thermal gradient values of approximately 1°F per 100 feet in depth. The intervening formation may be a material of high heat conductivity, such as clay. Lithologic logs indicate clays and sands are universally encountered in drilling in the Carrizo Plain area. Gravels are less common.

Well number three is located approximately 500 feet toward the north from well number four. Here, a clearly defined change in thermal gradient from 400 feet to 580 feet in depth indicates the location of a continuous layer of permeable material, underlain by a thermally less conductive material, such as clay or shale.

The data for well number five are consistent with those from driller's logs, which indicate that formations below 200 feet in depth consist of clay. The thermal gradient

measured between 60 feet and 170 feet in this well is 0.9°F . This is near the range of the average geothermal gradient for the Earth. It is unlikely that this interval contains much permeable material.

Well number seven was drilled near the shore of Soda Lake to a depth of 1,874 feet. According to the driller's log, it produced only 75 gallons per minute (gpm) with 672 feet of drawdown. The poor water-producing capability of this well is suggested in Figure 6.4 by the consistent thermal gradient of 1.75°F per 100 feet of depth.

Well number eight is located approximately 200 feet east of well number seven. The 60-foot to 135-foot interval of this well consists of permeable sediments, as indicated by the thermal gradient of 0.7°F per 100 feet (Figure 6.5). Below 135 feet, high values of heat conductivity indicate that there is little permeable material. At 580 feet in depth, the diminished slope of the curve may be due to high permeability, or to an obstruction in the well.

Method of wireline logging of boreholes

Wireline logs available for boreholes in the area of investigation were interpreted to augment the hydrogeologic information. The logs were useful for correlating sedimentary beds by providing information on the type of material of which a bed is composed, and the location of bed

boundaries. The logs available recorded spontaneous potential and electrical resistivity of formations encountered in the borehole.

Wireline logging results and interpretation

Wireline logs of different types were analyzed for four wells. For two of the logs (Figures 7.1 and 7.2), the resistivity of the zone near the borehole was measured by using a point resistivity probe. Zones more distant from the borehole were measured with a six-foot lateral electrode configuration. Two of the logs were produced using short normal, long normal, and lateral electrode configurations for shallow, moderate, and deep investigation, respectively.

For the northwestern well, the resistivity of the formations encountered is greater than the resistivity of the invaded zone at all depths (Figure 7.1). The difference is approximately 10 ohms m^2/m from 0 feet to 150 feet in depth, and approximately 16 ohms m^2/m from 150 feet to 385 feet in depth. The interval from 225 feet to 280 feet in depth displays relatively high resistivity values for zones distant from the borehole. The magnitude of point and lateral resistivity values, and the difference between the two, are diminished for the 385-foot to 450-foot interval. The SP curve is relatively straight, and positive in deflection from the 40-foot to 100-foot interval. The drift

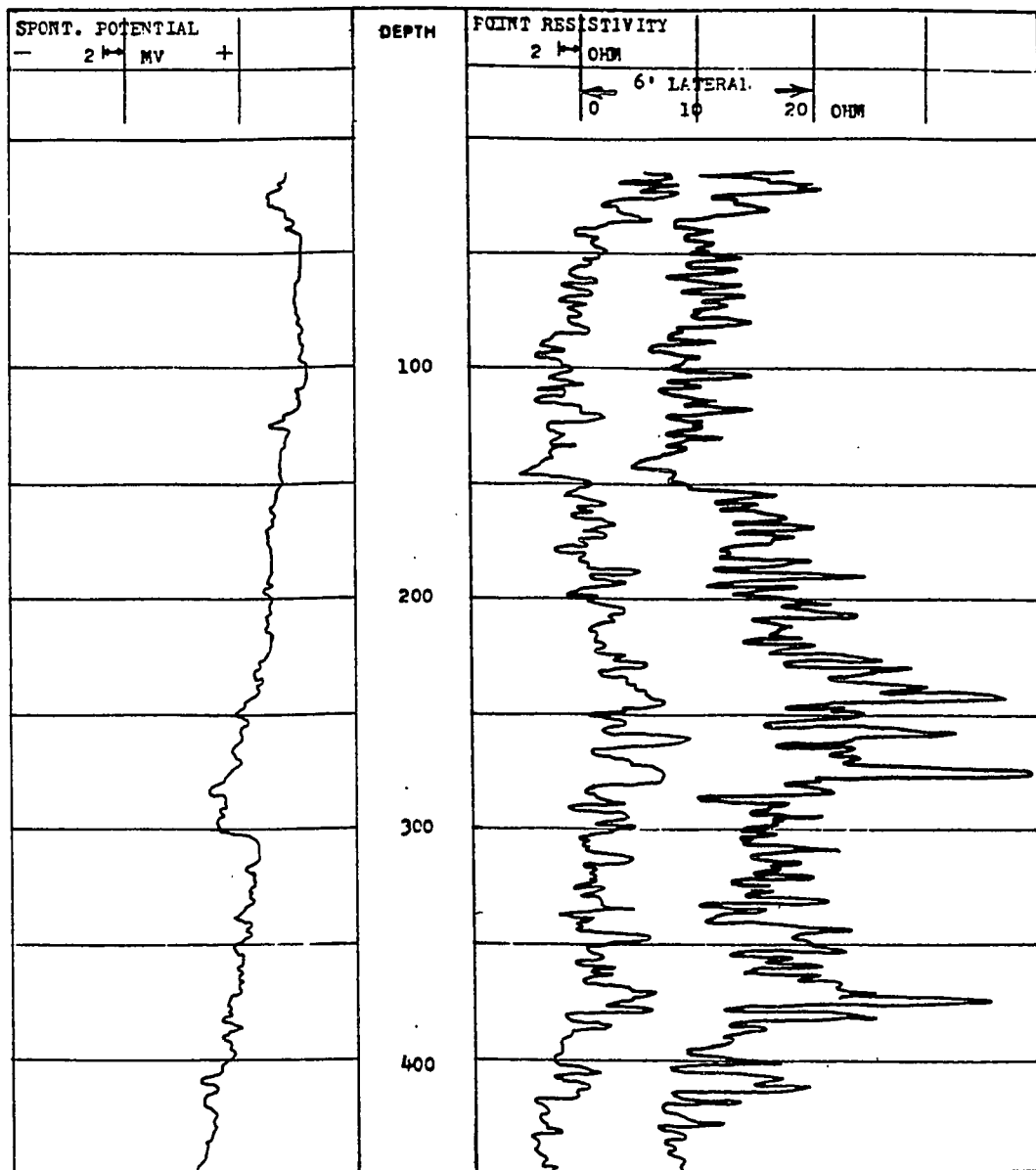


Figure 7.1. Electric log of well number 1. Fresh water is indicated by highest formation resistivities in the 225-foot to 285-foot, and the 360-foot to 380-foot intervals.

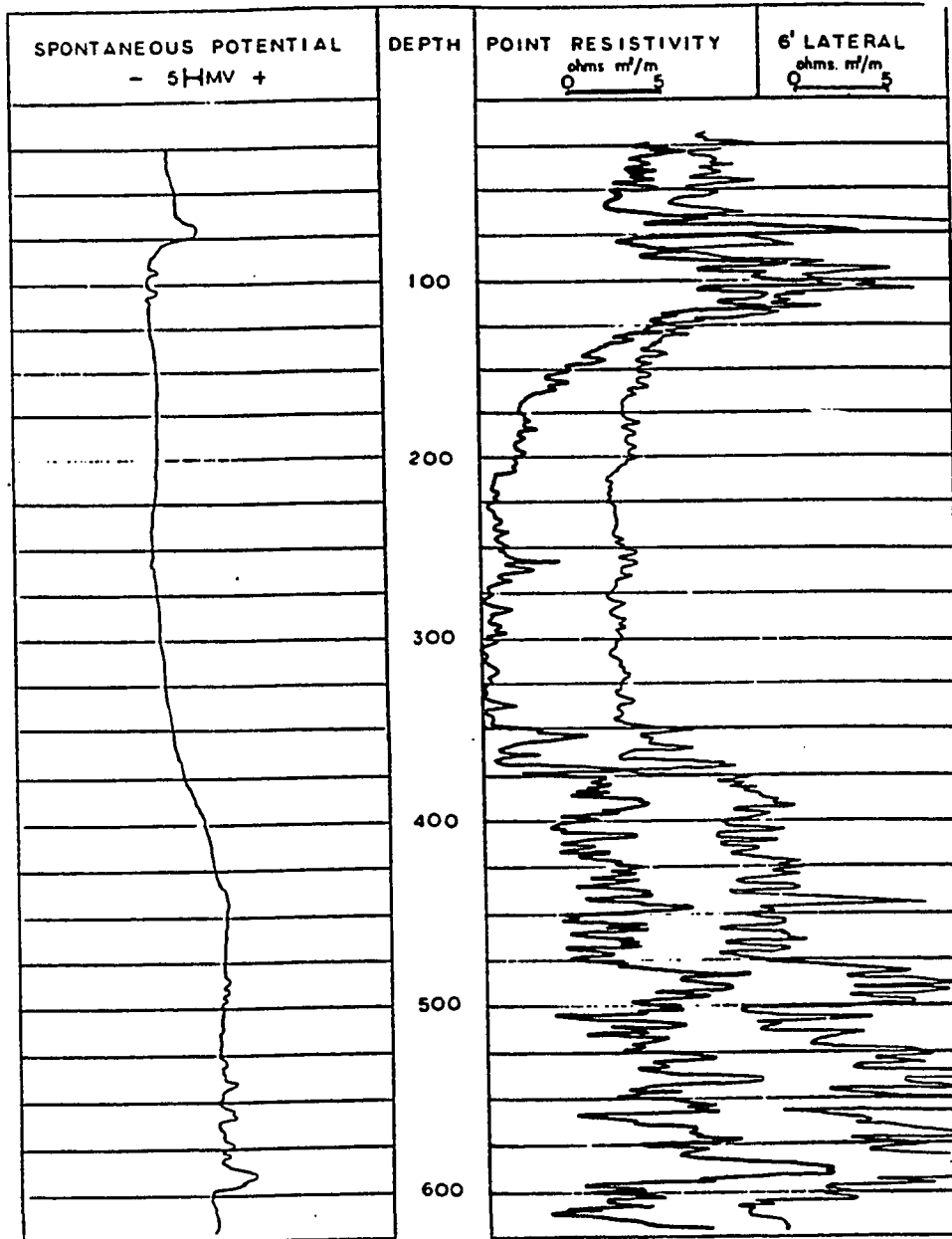


Figure 7.2. Electric log of well number 3. Lower resistivity and smoother curves for the 150-foot to 350-foot interval is interpreted as mostly clay. The most productive aquifer probably occurs at the 350-foot to 600-foot interval.

is toward the negative at depths greater than 110 feet.

The uniform deflection to the right of all three curves within a given depth interval, combined with the driller's description, provided an indication of the presence of groundwater with salinity lower than that of the borehole fluid. This relationship is useful only if the magnitude of the SP deflection is in excess of the normal background noise level of about ten millivolts for the specific beds of interest (personal communication, GeoHydroData). For well number one, the SP curve is not definitive within that parameter. The six-foot lateral curve shows greatest resistivities, indicating a high probability of available fresh water, in the 225-foot to 280-foot and in the 360-foot to 380-foot intervals. The 150-foot to 225-foot interval shows moderately elevated resistivity values for the six-foot lateral measurement. The sharp variations in resistivity which create the angular appearance of the curves may be caused by discrete sand and clay interbeds characteristic of the Carrizo Plains area. The driller's log for well number one describes the 210-foot to 310-foot interval as sand and cemented sand. The 350-foot to 385-foot interval is described as sand in the driller's log. Thus, the 225-foot to 285-foot and the 360-foot to 380-foot intervals are interpreted as the major water-producing zones of well number one.

The electric log of well number three (Figure 7.2) displays a fifteen-millivolt deflection of the SP curve between 65 feet and 85 feet in depth. The deflection of the SP curve correlates with excursions to the right of both resistivity curves. This suggests the presence of the shallowest water-bearing strata. These strata appear to extend to approximately 120 feet in depth. The deeper 120-foot to 350-foot interval is characterized by lower resistivity values and smoother curves. The strata at depths greater than 350 feet are associated with irregular resistivity curves having elevated resistivity values. The SP curve for this depth interval is irregular, indicating the presence of sand-shale or sand-clay interfaces. This interpretation correlates well with the lowered thermal gradient shown in Figure 6.1, and with the driller's report of sands from the surface to 140 feet in depth and from 360 feet in depth to bottom. Thus, the major water bearing zones in well number three are interpreted to exist at the 375-foot to 610-foot interval, and at the 60-foot to 120-foot interval of depth.

The electric log recorded for well number five (Figure 7.3) shows prominent "reversals". Reversals are graphic locations at which the SP curve is at minima for the depths at which the resistivity curves are at maxima. Reversals are caused by a liquid junction potential, and indicate the

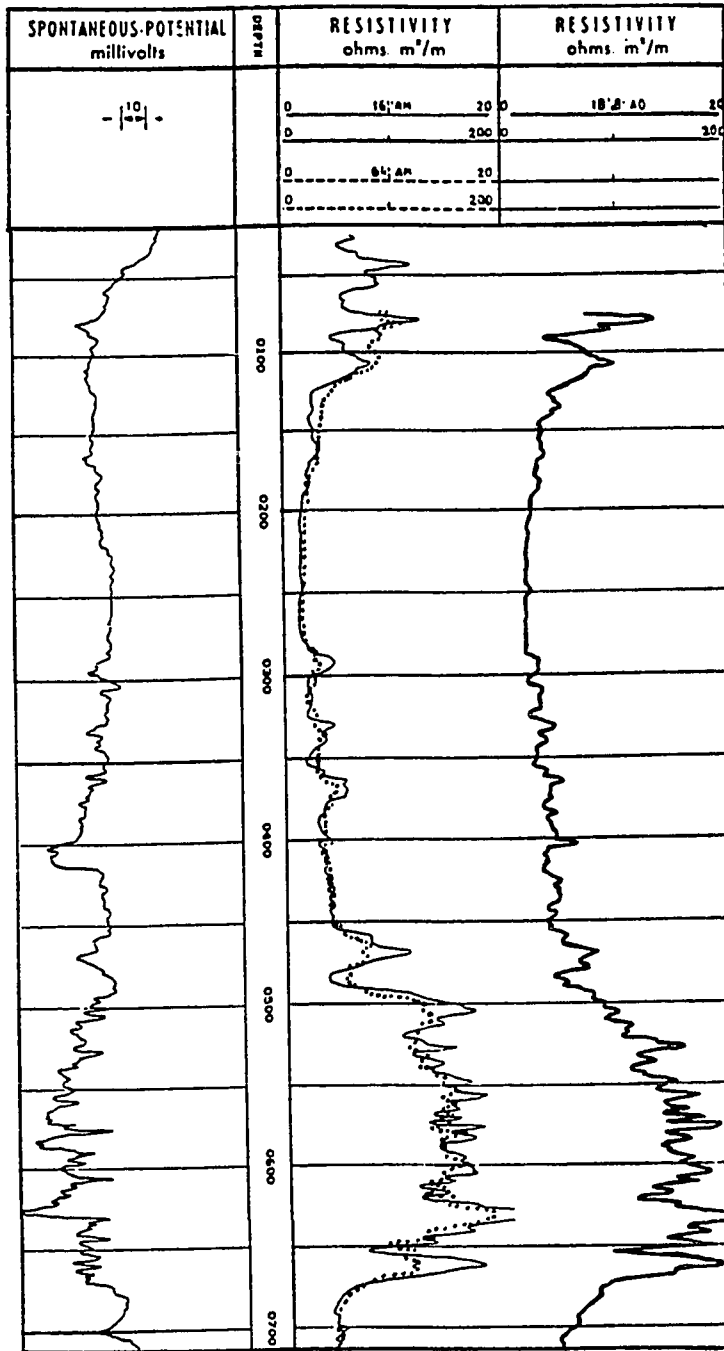


Figure 7.3. Electric log of well number 5. Clays are indicated for the 180-foot to 280-foot interval. Brackish formation water is indicated beneath the clays.

presence of formation fluid high in ionic concentration. Such reversals are evident at 80 feet, 290 feet, and 470 feet in depth. The broad trend of the curves between 480 feet and 700 feet in depth exhibits the same reversal. The curves vary little in the 180-foot to 280-foot interval. This interval is interpreted as the location of an impermeable clay stratum because of its consistent and low resistivity, and because of minimal variation in SP values for the interval. The angular irregularity of the curves between 480 feet and 700 feet in depth suggests the existence of clay or shale beds interbedded with sands or gravels. The lower values of resistivity for the long normal curve relative to those for the short normal curve in this zone suggests the formation water is more saline than the borehole fluid.

Well number eight is located approximately 500 feet southeast of well number five, on the east bank of a channel which conducts flood runoff to Soda Lake. The electric log for well number eight (Figure 7.4) exhibits deflections in the SP and resistivity curves of magnitude and direction similar to the pattern of the log for well number five. This provides a correlation of bedding boundaries for the two boreholes. However, the log for well number eight indicates fresh water for the 585-foot to 625-foot interval. The deep-investigation long normal curve

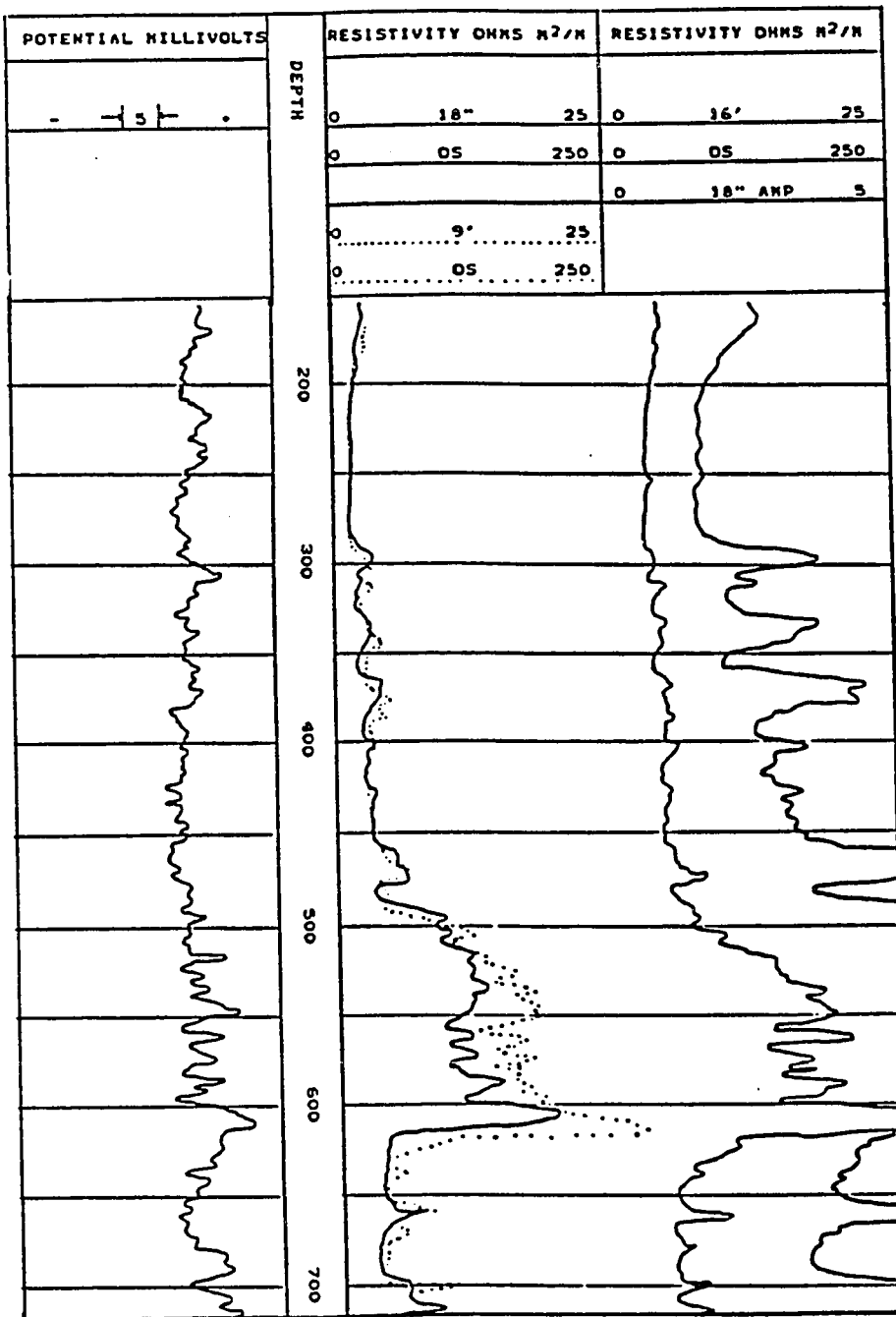


Figure 7.4. Electric log of well number 6, indicating a fresh water sand formation located between 525 feet and 625 feet in depth.

shows resistivities greater than those for the short normal curve throughout the interval. Comparison with the SP curve shows no reversals for the interval. The contradiction between the electric logs is probably not related to changes in lithology, because the similarity of curves suggests little stratigraphic difference between the two boreholes. Other factors which may cause the contradiction include logging instrument error and differences in drilling methods, both of which can affect the ability to obtain accurate information.

The electric log produced for well number seven, located near the shore of Soda Lake, shows reversals at all depths (Figure 7.5). The SP curve is nearly a mirror image of the short normal resistivity curve. Below 500 feet in depth, the long normal resistivity values are less than those for the short normal curve, indicating formation water of greater ionic concentration than the borehole fluid. These observations are consistent with the report of 27,000 parts per million total dissolved solids for this location (Kemnitzer, 1967). The low resistivity of the short normal and long normal curves, and the minimal variation of the SP and the resistivity curves are interpreted as reflecting predominantly clay and shale to 500 feet in depth. Other data indicating the poor quality and low quantity of water available at this location include a driller's report citing

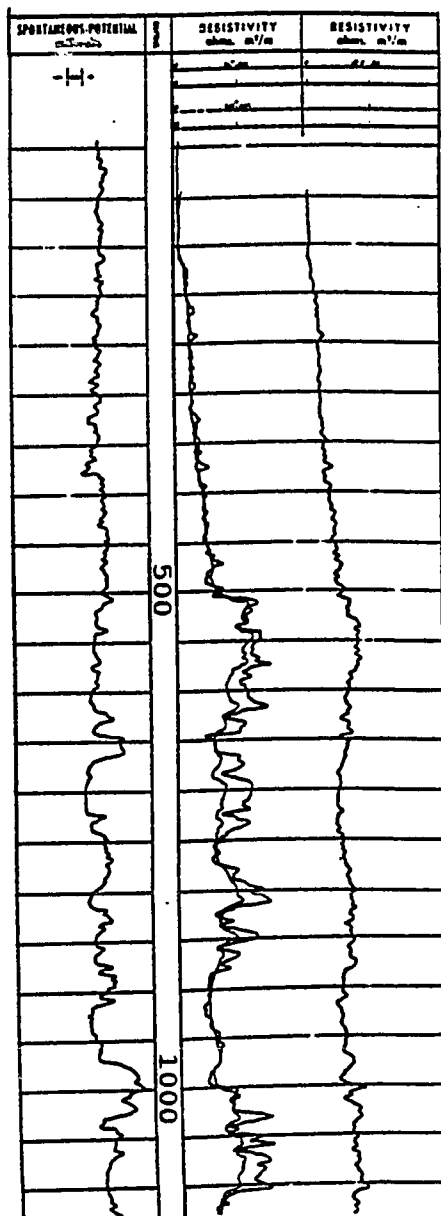


Figure 7.5. Electric log of well number 7. Mirror-like reflection of SP and resistivity curves indicates water of elevated ionic concentration.

a pump test which produced 75 gallons per minute, with 634 feet of drawdown. The thermal log for this well (Figure 6.4) indicates no zones of elevated heat conductivity. This location is interpreted to contain formations yielding brackish water in low quantities at depths ranging from the surface to 1,100 feet.

Piezometric levels

A contour map of the piezometric surface in the area of investigation was constructed to provide a base of data for more accurate interpretation of borehole and magnetic measurements (Table 5). The shape of the piezometric surface (Figure 8) indicates that groundwater flow is from the northwest to the southeast, with steepest head gradients near the mountain front. Depth to static water level varies from approximately ten feet near the center of the area to seventy feet on the southwestern mountain front. Water level information for the eastern part of the area is limited. Several dry wells were located there. Residents in the eastern half of the study area report that boreholes are often dry and that water produced is hard. The piezometric surface slopes more gently southwestward than does the topographic surface. The depth to static water level in wells in the southwestern mountain slopes is greater than that in the central plain. At the southernmost point of the

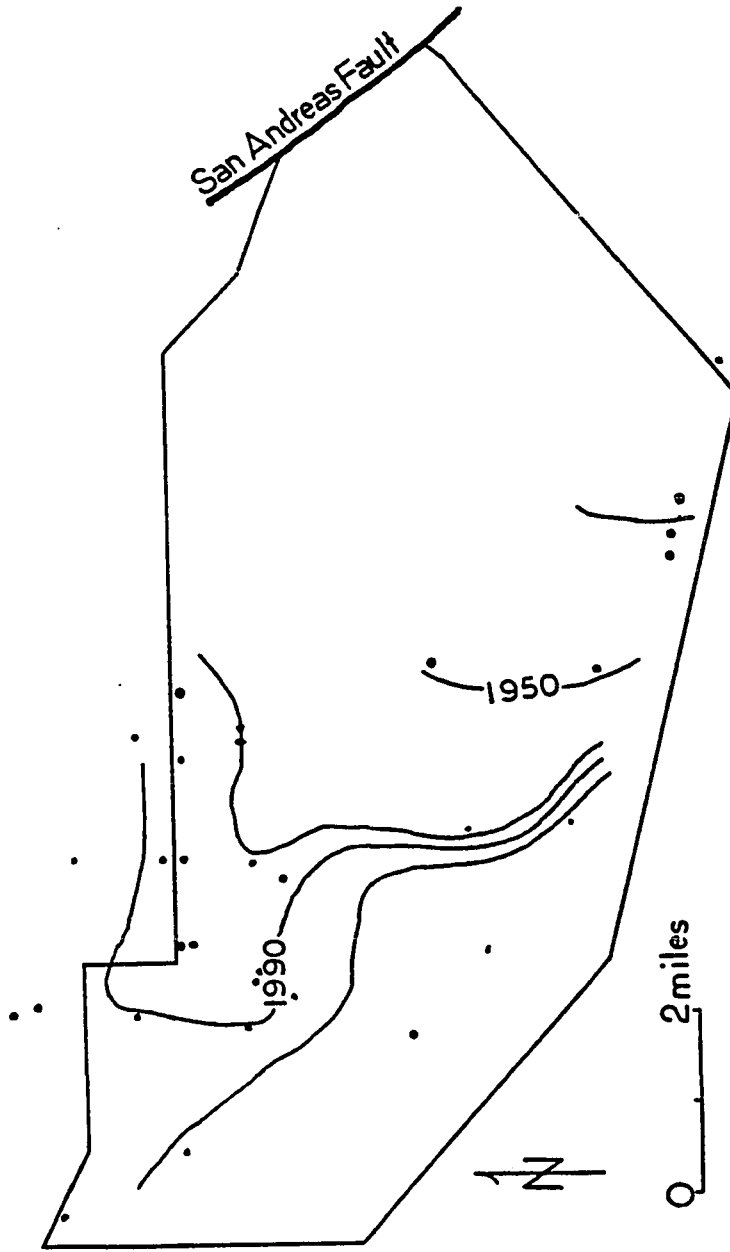


Figure 8. Map of the area of investigation, with lines of equal elevation of the piezometric surface. Measured as feet above sea level in July, 1989. Contour interval: 20 feet.

TABLE 5. Measurements of static water level or dry bottom of 31 wells abandoned or not pumped within the previous 24 hours. Elevations are feet above sea level, from USGS 7½-minute quadrangle maps. An explanation of the California well numbering system is given with Figure 9.

<u>Date</u>	<u>State well number</u>	<u>Surface elevation (feet)</u>	<u>Water level elevation (feet)</u>
7/18/89	28S/18E31K	2168	2154
7/18/89	29S/18E11J	2068	2041
7/12/89	29S/18E16M	2082	2052
7/18/89	29S18E28K	2024	2002
7/12/89	29S18E30L	2040	2006
7/11/89	29S18E33L	2003	1989
7/12/89	29S18E34A	2027	1996
7/11/89	29S18E35N	1997	1970
7/29/89	30S18E1A	2039	1973
7/12/89	30S18E1D	2006	1977
7/29/89	30S18E1L1	1988	1971
7/29/89	30S18E1L2	1990	1967
7/28/89	30S18E2N	1986	1970
7/11/89	30S18E3D	1991	2025
7/11/89	30S18E4P	2025	1990
7/11/89	30S18E4R1	2011	1992
7/11/89	30S18E4R2	2016	1990
7/11/89	30S18E6D	2065	2012
7/13/89	30S18E9B	2021	1994

Table 5 (continued):

<u>Date</u>	<u>State well number</u>	<u>Surface elevation (feet)</u>	<u>Water level elevation (feet)</u>
7/11/89	30S18E10A	1990	1978
7/22/89	30S18E16M	2170	2090
7/11/89	30S18E22D	2190	2105
7/11/89	30S18E23C	2019	1967
8/2/89	30S18E26B	2048	2020
7/31/89	30S18E36M	2017	1979
7/31/89	30S19E30E	1975	1946
7/31/89	30S19E32F	2020	1934
7/31/89	30S19E32G	2000	1932
7/31/89	30S19E32J	1960	1928
Dry hole:			
	30S20E18J	2180	2408

area, represented by the apex of the boundary corner, the static water level is approximately one foot in depth. This point is located approximately 2,000 feet from the shoreline of flooded Soda Lake during seasons of above-normal rainfall.

X D	C	B	A
E	F	G	H
M	L	K	J
N	P	Q	R

28

Figure 9. California water well identification system. Well example shown at X is the second well drilled on the northwest quarter of the northwest quarter of section 28, township 30 south, range 18 east. The state number is 30S/18E28D2.

DISCUSSION

A review of the magnetic data, piezometric data, and drillers' logs suggests that the previously-mapped fault zone located in the northwestern part of the area of investigation extends beneath the valley sediments. The area has good quality groundwater in supplies exceeding 100 gpm, according to drillers' reports of air-lift tests. Lithologic logs in this western area show no consistency for correlation of beds. The contour map of total magnetic intensity shows an anomaly at the northwest end of the area of investigation. The linear zone representing this anomaly has approximately the same trend and location as the zone of two faults mapped through outcrops bordering the alluvial plain. The anomaly is interpreted as an extension of the mapped faults through the basement rock. Magnetic profiles oriented approximately perpendicular to the zone show inflection points in approximately the same area as the interpreted fault zone. The 1990-foot isopiestic line on the piezometric surface contour map shows a subparallel alignment along a flattened segment in approximately the same area. Groundwater flow may be retarded by an argillaceous shear zone associated with the fault(s). There is no evidence of faulting in the surficial sediments, but the shear zone may displace subsurface Pleistocene sediment.

The anomaly in the southern part of the area of investigation is interpreted as a basaltic dike. The magnitude of the anomaly suggests that it is lithologic rather than structural, and previous workers have noted the abundance of basaltic dikes in the local formations. This feature is of little importance to the area's hydrogeology; water in the area is of inferior quality for residential or industrial use.

The combined interpretation of electric logs, thermal logs, and drillers' logs indicates the presence of a permeable sand bed in the central part of the area of investigation, including the area around well number three and well number five. The depth to the top of the bed ranges from approximately 200 feet to 500 feet. The data of well number one indicate that the strata at depth of less than approximately 190 feet are predominantly clay, and that those at greater depths are predominantly sand and cemented sand. The electric log and driller's log are the basis for this interpretation. The clay strata in this well may be equivalent to those of wells three, four and seven. This conclusion is uncertain, because well number one is approximately 160 feet shallower than the others. The top appears to be approximately 380 feet in depth at well number three and 480 feet in depth at wells number four and seven. The sands are mostly medium to fine grained, and are usually

interbedded with clays and silts. The permeable bed is overlain by a clay layer which is interbedded with thinner silt and sand layers. This impermeable bed is well-defined on the electric logs of wells three, four and seven. The top of the bed is approximately 150 feet in depth at well number three, and 200 feet in depth at wells number four and seven.

Water quality variations in the area of investigation are in part due to the geology of the area. Concentrations of total dissolved solids (TDS) increase from northwest to southeast and from southwest to northeast. Gypsum mines are located along the San Andreas fault. Evaporites associated with the gypsum which have accumulated along the San Andreas fault and in Soda Lake are concluded to be the cause of the deterioration of water quality in the direction of these geologic features. The amount of TDS in the water correlates with the length of time the groundwater is in contact with these minerals. Residents report that in some areas the mineral content of the well water increases with increasing depth. This may be caused by clay interbeds which tend to keep younger water at shallower depths. Electric logs show the trend of increasing TDS in the direction of Soda Lake, as discussed earlier.

CONCLUSIONS

This investigation resulted in several conclusions regarding the hydrogeology of the area. The fault zone located in northwestern end of the area extends farther northeasterly than previously mapped. A basaltic dike is located beneath the surface in the southern part of the area. A southeastward-dipping permeable sand bed 200 feet to 500 feet below the ground surface is located in the central part of the area of investigation. Groundwater quality deteriorates in a southeastward direction due to the increased TDS concentration contributed from evaporite dissolution.

BIBLIOGRAPHY

GENERAL GEOLOGY

- Bartow, J.W., 1988, Geologic map of the northwestern Caliente Range, San Luis Obispo County, California: United States Geological Survey Open-File Report 88-691.
- Bentall, Ray, ed., 1963, Methods of collecting and interpreting ground-water data: United States Geological Survey Water-Supply Paper 1544-H.
- California Department of Water Resources, 1958, San Luis Obispo County Investigation: bulletin 18, volumes I and II.
- Chipping, David H., 1972, Early Tertiary Paleogeography of Central California: The American Association of Petroleum Geologists, v. 56, no.3, p. 480-493.
- Davis, T.L., Lagoe, M.B., Bazeley, W.J.M., Gordon, Stuart, McIntosh, Kirk, and Namson, J.S., 1988, Structure of the Cuyama Valley, Caliente Range, and Carrizo Plain and its significance to the structural style of the southern Coast Ranges and western Transverse Ranges, in Tertiary tectonics and sedimentation in the Cuyama basin, San Luis Obispo, Santa Barbara, and Ventura Counties, California: Society of Economic Paleontologists and Mineralogists, Pacific Section, v. 59, p. 141-158.
- Dibblee, Thomas W., Jr., 1973, Stratigraphy of the Southern Coast Ranges near the San Andreas Fault from Cholame to Maricopa, California: United States Geological Survey, Professional Paper 764, 45 pp.
- Dobrin, Milton B., Savit, Carl H., 1988, Introduction to geophysical prospecting: McGraw-Hill, Inc., 867 pp.
- Eichel, Marijean H., 1971, The Carrizo Plain, a geographic study of settlement, land use and change: San Jose State College thesis, 71 pp.
- Freeze, R. Allan, Cherry, John A., Groundwater: Prentice-Hall, Inc., 604 pp.

- Galehouse, Jon S., 1967, Provenance and Paleocurrents of the Paso Robles Formation, California: Geological Society of America Bulletin, v. 78, p. 951-978.
- Graham, S.A., McCloy, C., Hitzman, M., Ward, Jr., Turner, R., 1984, Basin evolution during change from convergent to transform continental margin in central California: AAPG Bull., v. 68, no. 3.
- Greene, Gary H., 1977, Geology of the Monterey Bay Region: United States Geological Survey Open File Report 77-718, 197 pp.
- Kemnitzer, William J., 1967, Ground water in the Carrizo Plain, San Luis Obispo County, California: unpublished, 75 pp. (held at California Polytechnic State University, San Luis Obispo).
- Lagoe, Martin B., 1985, Depositional environments in the Monterey Formation, Cuyama Basin, California: Geological Society of America Bulletin, v. 96, p. 1296-1312.
- Lima, Joseph M., 1975, Rainfall and temperature analysis of the Carrizo Plain, San Luis Obispo County, California: Senior Project, California Polytechnic State University, 159 pp.
- Lindh, Allan, et. al., 1985, Parkfield prediction program: United States Geological Survey, Open File Report 86-580, pp. 34-38.
- Ross, Donald C., 1978, The Salinian Block--A Mesozoic Granitic Orphan in the California Coast Range, in Mesozoic Paleogeography of the Western United States: Pacific coast Paleogeography Symposium 2, Society of Economic Paleontologists and Mineralogists, Pacific Section, p. 509-521.
- Sieh, Kerry E., Jahns, Richard H., 1984, Holocene activity of the San Andreas fault at Wallace Creek, California: Geological Society of America Bulletin, v. 95, p. 883-896.

MAGNETICS

- Birch, Francis S., 1984, Bedrock depth estimates from ground magnetometer profiles: Groundwater, v. 22, no. 4, p. 427-432.

- Breiner, S., 1973, Applications manual for portable magnetometers: Geometrics, Inc.
- Grasty, James W., 1988, A gravity and magnetic study of the Armstrong Ranch area, Monterey County, California: San Jose State University thesis, 87 pp.
- Nettleton, L.L., 1971, Elementary gravity and magnetics for geologists and seismologists: Society of Exploration Geophysicists, monograph series, no. 1, 121 pp.
- Nettleton, L.L., 1976, Gravity and magnetics in oil prospecting: McGraw-Hill International Series in the Earth and Planetary Sciences, 452 pp.

GEOHERMAL

- Bair, E. Scott, Parizek, Richard R., 1978, Detection of Permeability Variations by a Shallow Geothermal Technique: Groundwater, Vol.16, No. 4, p. 254-263.
- Birman, Joseph H., 1969, Geothermal exploration for ground water: Geological Society of America Bulletin, v. 80, p. 617-630.
- Cartwright, Keros, 1974, Tracing shallow groundwater systems by soil temperatures: Water Resources Research, v. 10, no. 4, p. 847-855.
- Driscoll, F.G., 1989, Groundwater and Wells: p. 196-200.
- Lovering, Thomas S., Goode, Harry D., 1963, Measuring Geothermal Gradients in Drill Holes Less Than 60 Feet Deep, East Tintic District, Utah: United States Geological Survey, Bulletin 1172., 48 pp.
- Schneider, Robert, 1962, An application of thermometry to the study of ground water: USGS Water-Supply Paper 1544-B.

BOREHOLE GEOPHYSICS

- Campbell, Michael D., and Lehr, Jay H., 1973, Water Well Technology: McGraw-Hill, New York, 681 pp.
- Keys, W.Scott, MacCary, L.M., 1971, Application of Borehole Geophysics to Water-Resources Investigations: USGS Techniques of Water-Resources Investigations, Chapter E1, Book 2, 126 pp.

Lovering, Thomas S., Goode, Harry D., 1963, Measuring Geothermal Gradients in Drill Holes Less Than 60 Feet Deep, East Tintic District, Utah: United States Geological Survey, Bulletin 1172., 48 pp.

Newman, Joseph L., no date, Water well geophysical logs, Welenco, Inc.

Patten, Eugene P., Jr., Bennett, Gordon D., 1963, Application of electrical and radioactive well logging to ground-water hydrology: USGS Water-Supply Paper 1544-D.